© von Karman Institute for Fluid Dynamics
Waterloosteenweg 72 – 1640 Sint-Genesisu-Rode

Dear reader,

The electronic document attached is protected by copyright laws.

This article may be used for research, teaching and private study purposes. Any substantial or systematic reproduction, redistribution, reselling, loan, sub-licensing, systematic supply, or distribution in any form to anyone is expressly forbidden.

Please do not distribute the document to third parties outside your workgroup as under current copyright law it is only intended for your personal scientific use. If you do not comply with the above conditions of use, you may be held liable for copyright infringement.

VON KARMAN INSTITUTE FOR FLUID DYNAMICS

LECTURE SERIES 1984-03

DIGITAL IMAGE PROCESSING IN FLUID DYNAMICS

MARCH 5-9, 1984

INSTANTANEOUS CONCENTRATION AND VELOCITY MEASUREMENTS THROUGH LASER VISUALIZATION ASSOCIATED WITH A DIGITAL PROCESSING SYSTEM

J.P. SCHON - ECOLE CENTRALE DE LYON ET
UNIVERSITÉ DE ST ETIENNE, FRANCE

1. INTRODUCTION

In the present lecture, we will focus on two applications of image processing in fluid dynamics. However, we must not forget that the physical processes involved in any technique have to be examined very carefully to test the validity of the results.

An image is the result of quite a number of physical processes which can be quite complicated. That was certainly one of the reasons that flow visualization was employed, until recently, to get only results.

Images of flows can be obtained in a great variety of cases ; for example, the variation of the optical index with density is used by SCHLIEREN or other techniques, the radiative emission can be recorded by infrared cameras for hot walls or for flames.

In most of the cases, the flow is seeded by particles which are illuminated and the images are obtained by recording the light diffused by this particles.

Lasers enable us to illuminate these particles with enough energy to obtain images of acceptable quality, but we must keep in mind that the information recorded on an image is always biased by many phenomena.

So, in this paper we will first describe the visualization technique we used. The application to concentration measurements will be discussed in the second part. Problems linked to velocity measurements will be developed in the third part and we will conclude by giving some elements for future work.

II. DESCRIPTION OF THE VISUALIZATION TECHNIQUE

The technique is one of the versions of the "laser tomography technique" and consists to sweep a sheet of the flow by a laser beam associated to rotating mirrors (figure 1). This idea due to F. DANEL (A.I.D. - ZIRST - GRENOBLE) (see SCHON et Al. - 1979) has the advantage to concentrate a great quantity of energy on the particles at a known frequency. Several groups use vibrating mirrors but the sweep velocity is not constant (GANDEMER, PERRIER).

The expanded beam technique (use of a cylindrical lense to expend the been) which is used here at Von Karman, has the advantage to be more simple to use but does not concentrate the energy as much.

In our case, as we work in air with little particles (1 µm), we use a 5 Watts ARGON laser. The rotating device is made of 16 mirrors. The sweeping frequency can be varied from 10 to 1000 Hz. The thickness of the beam in the observation region is about 2 mm.

Two procedures can be used :

- if many particles are present in the flow and if only one sweep is used, the diffused light is linked to the local particle number so concentration measurements are possible.
- if few particles are in the flow and several sweeps are used, then the trajectories of these particles can be recorded and velocity fields can be determined.

The light emitted by the particles is recorded on photographic films (faster response than classical video devices, more analog information stored). Each photograph or part of the photograph is digitized on a EYECOM II System associated to several computers (figure 2), on which the digital processing is performed.

III. PHYSICAL PROCESSES

III.1. Particle behaviour

As the flow is seeded by particles, one has to study the dynamics of particles in a flow. This is in peculiar very important in the case of diffusion studies. In effect, even if the particles are small and if their velocity difference is small with the associated fluid particle, the correlation loss can be important when time increases. This effect was emphasized by CSANADY. (1963) is less important when local velocities have to be determined because no "integral" effect comes into play. Not very much information is available on the particle behaviour in turbulent flow because of the complexity of the phenomena .(SNYDER and LUMLEY (1971),WELLS and STOCK(1983))

In usual cases, when the KNUDSEN number is small (ratio of the mean free run ℓ of the molecules to the diameter of the particles (for d = 1 µm Kn = 6.4 10^{-2} for air at 15°C and 1 atm.) ;

- if the particle density is small so that the interaction between particles can be neglected,

- if at last the size of particles is small compared to the smallest scales of the flow (Kolmogorov scales),

the velocity can then be considered as constant in the vicinity of the particle. The flow around the particle is in the Stokes regime in most of the practical cases. In effect, if V_r is the relative velocity of the particle, the Stokes regime is valid for a Reynolds number $Re_r = \frac{V_r\, d}{\nu}$ lower than .5. For a 1 µm particle in air this corresponds to V_r = 7.5 m/s, which is always realized.

The equation governing the dynamics of the particles are given by a very complex expression (see for exemple LUMLEY, 1957).

$$\frac{d\vec{V}}{dt} = \alpha(\vec{U} - \vec{V}) + \beta\frac{d\vec{U}}{dt} + \gamma\int_{-\infty}^{t}\left(\frac{d\vec{U}}{d\tau} - \frac{d\vec{V}}{d\tau}\right)\frac{d\tau}{\sqrt{t-\tau}} + \delta\vec{g}$$

with :

$$\alpha = \frac{36\mu}{d^2(2\rho_p + \rho)}$$

$$\beta = 3\rho/(2\rho_p + \rho)$$

$$\gamma = \frac{18}{d(2\rho_p + \rho)}\sqrt{\frac{\mu\rho}{\pi}}$$

$$\delta = 2(\rho_p - \rho)/(2\rho_p + \rho)$$

V particle velocity

U fluid velocity

ρ fluid density

ρ_p particle density

d particle diameter

μ viscosity

$\frac{d}{dt}$ total derivative

LUMLEY (1957) showed that if the particles are small and if the characteristic time real $1/\alpha = a$ is small compared to the Kolmogorov time scale then the previous equation reduces to :

$$\frac{d\vec{v}}{dt} = \frac{1}{a}(\vec{U} - \vec{v}) + \vec{g}$$

if $\rho_p >> \rho$ $\quad a = \frac{d\rho_p}{18\mu}$

a is linked to the free fall velocity $V_L = ag$. Table 1 gives some values of the free fall velocity for different particles.

If we consider that trajectory crossing effects are negligeable if $U >> V_L$, 1 µm particles can be considered as passive and their concentration C described by the classical diffusion equation :

$$\frac{\partial C}{\partial t} + U_j \frac{\partial C}{\partial x_j} = D \frac{\partial^2 C}{\partial x_j \partial x_j}$$

D is the apparent diffusivity due to Brownian motion.

$$\mathcal{D} = \left(1 - \frac{\rho}{\rho_p}\right)\frac{kT}{3\pi\mu d} \simeq \frac{kT}{3\pi\mu d}$$

k : Boltzman constant

T : absolute temperature

Different values of D are given in table II. It is of interest to notice that the values of diffusivity leads to high Schmidt numbers ($\sim 10^5$) compared to gaz in air, or compared to the air Prandtl number. This phenomena can be important in some cases.

All the previous analysis shows that the dynamics of particles in turbulent media is very complicated and in fact very little is known about the decorrelation between the particle and the fluid particle associated at the release point. A wide field of research is open especially with image processing techniques to get information on these phenomena.

III.2. Seeding of the fluid

We want just recall that the seeding of the flow is a relatively simple problem when used for laser doppler anemometry. However, if the flow is seeded for quantitative visualization, more care is needed. As shown in the previous section, the particles must be small and the concentration at the injection has to be constant. It is convenient to produce a nearly monodispersed aerosol to get the same optical and dynamical response of each single particle. However, it is practically impossible at a reasonable cost. In our case, we used for diffusion experiments incence smoke produced by the system shown on figure 3 . For velocity measurements, aloxite particles of 4 µm or bubbles with helium were used (DRIVIERE-1982, MARTINE-1982).

The figure 4 shows the particle diameter histogram of the incense particles measured by a ROYCO LASER 256 particles counter. The diffusion of light by the particles is supposed to be linked to the concentration and will be discussed in the next section.

III.3. Scattering of light by particles

As the scattering of light by the particles is the physical phenomena used in most visualization techniques, some information on the phenomena is of interest.

Light scattering results from the interaction between radiation and matter. The energy level of the electrons is modified so light is remitted. The problem has been solved by MIE (1908) for a sphere with a given refraction index and submitted to a monochromatic plane wave. The MIE theory can be simplified for very big particles and for particles the diameter of which being lower than the wavelength of the light (RAYLEIGH-1899). A complete discussion of the theory based on Maxwell equations can be found in KERKER (1969), VAN DEN HULST (1957), BRICARD (1977). The intensity of the scattered light is a quite complex fonction of the particle diameter, the distance of the particle and the direction. For very small particles when the Rayleigh theory is applicable, the intensity varies a 6 power law of the particle diameter ($d < \lambda/10$). Unfortunately, the particles of smoke are not spherical so it is at the moment not possible to use the existing theories.

SINCLAIR and LAMER (1949) have verified experimentally that the light scattered by a volume which contains small particles is proportional to the number of particles. We will assume that this result applies also to non spherical particles, the dimensions of which are of the order of 1 μm. We assume also that the diameter repartition of the particles is independant from the concentration.

This last assumption will probably be false for long diffusion time because of the differences in dynamic behaviour due to trajectory crossing and apparent molecular diffusion.

The particle concentration has to be low enough to avoid particle interaction and to avoid attenuation of the light recorded by the camera by particles located between the light sheet and the camera.

For 1 μm particles at a concentration of 10^7 particles per cubic centimeter, these effects can be neglected. At last, we use the whole power of an argon laser, the fact that the energy is mainly at 488 nm and at 514 nm does not seem to be of importance.

III.4. Problems linked to the image recording

The light diffused by particles is recorded on a photographic film or on video system. In all the cases, lenses are used to focus the images, so the energy emitted by the particles is modified by the lenses. This modification is a function of the optical characteristics of the lenses and also of the angle of the object seen from the lens with the optical axe of the lenses. The relation describing this phenomena is :

$$E' = L \frac{u - F}{2uf} T.H \cos^4\theta$$

with E' exposure
L luminance
F focal length of the lens
f relative aperture of the lens
T lens transmittance
H vignetting coefficient ray
θ angle between the object ray and the optical axe
u lens image distance

So a significant attenuation can occur far from the center of the photograph.

The response of the photographic film is also of importance. The expure of the film leads to a darkening which can be defined by the density. The density is far from a linear function of the exposure (figure 5) and depends also from the development and the sensitivity of the film. It is of interest to note that the information that can be recorded even on a standard photographic film is large compared to the chemical sizes of digital images ($\sim$3000 x 3000) compared to 512 x 512).

The photographs are digitized by a vidicon camera associated to an analog to digital converter. Vignetting is also present on the lens of the camera and the camera response is not linear. However, the film is observed by transparence, so the effect of the video camera lens is opposite to the photo camera but the compensation is not complete, the lense being different.

We have shown that the different processes involved by the visualization are very complex and not well known so it is necessary to develop a technique of direct calibration which avoids to use too many crude assumptions

IV. PRODEDURE FOR INSTANTANEOUS CONCENTRATION MEASUREMENTS

To take the image, photography was prefered to video because of the better definition and because of the response of the standard video systems (25 images per second). The images are taken either with one or two NIKON F2 cameras or with cinema camera of 16 or 35 mm.

With the NIKON camera, sets of 250 images can be taken. As far as we know no significant variation in the laser intensity or on the seeding concentration could be determined. As the processing of the films can vary from one film to another, the calibration procedure has be performed for each simple film. We will describe the different stages of the procedure :

- image recording and digitalization
- correction of the defaults introduced by the optics and the sensors
- calibration of the image

IV.1. Image recording and digitalization

The particles which are illuminated by the 5W Argon laser scatter light which is recorded by mean of the NIKON Camera on a 400 ASA KODAK TRI X or a ILFORD HP5 film, we usually use a processing up to 1600 ASA which enables us to keep a resolution of about 50 lignes per

millimeter, which remains compatible with the digitalization resolution. The film has to be processed in very stable conditions to avoid variations in the film response between the different images. At the beginning of the film uniform test images are taken which are used for the calibration. The photo 1 shows an example of an image which is obtained. The digitalization is performed as already stated by an EYECOM Vidicon Camera associated with a fast A/D converter, the definition of the digital image beeing 512 x 640 x 8 bits. The scheme of the system is given on figure 2 . The calibration of the video system has to be regularly tested.

IV.2. Correction of the defaults of the image

As mentionned before several uniform images are taken at the beginning of the film;these images are taken and digitized in the same conditions than the flow images, so the digital images obtained reflect the defaults of the system. From these digital images, a correction image can be computed and all the other images are multiplied by this correction image. It is verified by use of false color that the background of the corrected images is nearly uniform (photo 2 and 3),

IV.3. Calibration

In the case where unsteady flow is studied (for example diffusion of puffs released from a point source), the relation between gray level and concentration cannot be determined so it is necessary to take first on the film a steady phenomena, for which the mean concentration field can be measured by a particle counter (ROYCO LASER SYSTEM). The addition these images enables the obtention of a mean image (photo 4), the gray levels of which are compared to the corresponding measurements of mean concentration. The calibration curve so obtained is non linear (photo 5). The calibration is applied to each instantaneous image and a new mean image is computed. If the new mean image is close to the calibrated mean image, the calibration can be considered as satisfactory. Usually, two successive calibrations are used to get acceptable results ($\sim$ 10 %). The calibration induces some loss of information due to the non-linearity as shown by the histogram of the photo 6.

After this rather complicated procedure, we can estimate that we have a set of images on which the grey level is linearly related to the particle concentration. It is now possible to process these images to get interesting results for fluid dynamics.

V. EXAMPLES OF STUDIES ON TURBULENT CONCENTRATION FIELDS

V.1. Turbulent round jet

The round jet was investigated with the method by BALINT (1982), a set of 310 "good" images could be selected among a big amount of pictures. The diameter of the jet is 30 mm and the exhaust velocity 5 m/s. This corresponds to a Reynolds number of about 10 000. The sweeping frequency is 60 Hz, so the linear velocity of the beam is of the order of ten times the maximum velocity. The deplacement of a particle during illumination is negligeable but 1/60 s elapses between the extreme points of the image. This is not important for one point statistics but introduces some bias for two points correlations.

On the photo 7, the mean concentration field of the jet is given. The RMS value of the concentration fluctuation and the cubic root of the third order moment are given on photos 8 and 9.

The RMS values of the concentration fluctuation is high compared to values found in the litterature for passive scalars (for a review see LOCKWOOD-1980). Two remarks can be made : the first is that their is a considerable scatter in the reported data, especially in the region near from the jet exhaust, the second is that the scatter is due on the one hand to Reynolds number effects and different limiting conditions (is is not possible for temperature to avoid completely heat fluxes in the nozzle), and on the other hand to the low molecular diffusivity of particles. A simple monodimensional conduction model computed of a sinusoïdal repartition of concentration evolves quite rapidly for temperature at high frequencies when there is no modification for particles. So, molecular diffusivity can reduce significantly the

RMS values for temperature compared to particles when the gradients are high which is the case for the region near the jet exhaust.

The third order moment shows that in the outer region of the jet, the concentration variations are more intense and spatially smaller than in the inner region.

Spatial correlations have been computed for different points of the jet (photos 10 and 11). In spite of the bias which is certainly present, some interesting conclusions can be derived from the correlation cards. In effect, alternative positive and negative correlation region are present and inclined with an angle of 45° with the axis of the jet. This is certainly to be related to the vortex pairing mechanism which induces turbulence in jets.

V.2. Diffusion from stacks in a wind tunnel simulation

The determination of the instantaneous concentration fields is of special interest for environmental studies in wind tunnel simulations. In effect, without going too much into details, the wind tunnel simulation of atmospheric phenomena at a scale of 1/500 implies that the time scale is reduced in the same ratio. So if one is not able to get "instantaneous measurement" concentration peaks which can be important in the field cannot be detected on the model. On the other hand, for a given industrial plant, the alarm network is obviously limited, so it can be of interest to determine the point probability of the concentration between a place equiped with a measuring device and any otherplace. The system has been used to define the characteristics of concentration fields for different cases of plumes or puffs emitted from a stack model in a wind tunnel. Photos 12, 13 and 14 show the effect of clift on an instantaneous plume, the mean concentration field and the RMS value of the concentration fluctuations.

In case of the release of a puff, the statistics can be obtained by a certain number of realisations of a short release. The evolution of the puff can be determined by its visualization at two different instants. This was done for different cases in our atmospheric tunnel and on photos 15 and 16.

We have computed the statistical mean concentration a two positions of the puff. The statistical root mean square is given on photo 17 and 18. The probability of occurence of a concentration higher than a given level can also be determined (photo 19 and 20). Dispersive characteristics of the flow can also be determined by comparison of the geometrical characteristics of the puff between two instants. Figure 6 gives for example the evolution of the surface ratio of the puffs as a function of concentration. Numerous other geometrical characteristics can be defined, (SCHON et Al. - 1984). (VEILLON 1982)

V.3. Other examples

The technique can also be used to define quite various fundamental features. For example, digital image processing has been used to characterize the boundary of a turbulent boundary layer (photo 21 to 23). The statistical characteristics of the boundary length vary with the transition device of the boundary layer. Digital filtering can also be used to characterize certain structures of the flow.

VI. VELOCITY MEASUREMENTS

We will limit ourself to the rotating mirror technique, a double pulse laser technique similar to the one developed by MEYNART is also under development.

The system was mainly used by MARTINE (1982) to study the flow in a convection chamber of the geometry of which is given on figure . As the velocities can be very small near neutralseeding particles have to be used. The technique used is the technique of DRIVIERE, HENRY (1981) consisting in soap bubbles inflated with an air helium mixture. The mean diameter of the bubbles has been measured on micro-photographs.

The mean diameter is .7 mm. The maximum value being 1.2 mm, the minimum .2. The different terms of the equation of the particle dynamics are no more negligeable except for the gravity term who is nearly equal to zero. But as the velocities are small and the bubble diameter is somewhat lower that the Kolmogorov microscale which is about 2 mm in this case.

The primitive technique has been improved to get at the same time the velocity and the direction of the particles. This was obtain through occultation of some of the sixteen mirrors to get sequences of three sweeps followed by two sweeps and at last one sweep. The photo 24 shows such sequences. The image is then enhanced by filtering and histogram broadening and at last binarised (photo 25). The existence of cells for the mean could no clearly be raised (figure 7), and the root mean square values of the fluctuations are similar to those got by other authors (fig. 8).

This technique is however difficult to apply to high speed flow because of the bias effect. To determine the velocity of a particle, this particle must be illuminated two times to get successive positions of the particle (figure 9). If the particle is crossing the illumination sheet this is not always the case and even the determination of the mean velocity projection on the sweeping sheet can be affected.

Even if the mean velocity is in the plane, the turbulence can prevent the particle to remain in the sheet, for example, if we admitt that the lateral fluctuation v follows a gaussian probability law, if the frequency is f and the sheet thickness d the maximum trajectory angle θ_{max} is given by :

$$tg\ \theta_{max} = \frac{d f}{\overline{U}}$$

considering the limit case with just two points in the flow. If $\theta > \theta_{max}$ no particle with such trajectory will be sampled. If $\overline{U}$ = 1 m/s and if $v'/\overline{U}$ = 10 %, nearly all the trajectory angles are sampled if d = 1 mm, f = 1000 Hz if U = 10 m/s and $v'/\overline{U}$ = 30 % only ~30% of the possible trajectories can be recorded.

CONCLUSION

The domain of application of image processing in fluid mechanics is so wide than no theoretical limits can be imagined. However the quality of the primitive image is very important, so the visualization technique has to be performed with care. Massive use of digital image processing will probably entrain a fairly different way of describing turbulent flows. Multivariable statistics adapted to these flows will certainly be developped. Methods for describing three dimensional instantaneous velocity and concentration fields by holographic or other methods are studied. In all the cases, however, a great amount of data has to be handled. Samples of 1000 images are probably necessary for high order statistics, more definition is needed for quite a wide range of problems. So the real limits of these kind of methods are linked to the image processing performances and cost.

ACKNOWLEDGEMENTS

The work which has been done at the Ecole Centrale de Lyon is far from a "one man performance". Among those who participate actively to it, I thank M. AYRAULT, J.L. BALINT, O. DEBBARH, F. LADHARI, P. MEJEAN, J. MOLINES, R. MOREL, P. PERROUX, F. PRABEL and J. WALLACE. I thank also S. GUINAMARD for typing the text.

We acknowledge for financial support Electricité de France, DRET, Ministère de l'Environnement and European Community.

BIBLIOGRAPHY.

BALINT J.L. (1982)
"Application d'une méthode de visualisation laser et de traitement d'images à l'étude de la dispersion dans les écoulements turbulents",
Thèse Lyon

BRICARD J. (1977),
"Physique des aerosols"
rapport C.E.A. R4831.

CSANADY C.T., (1963),
"Turbulent diffusion of heavy particles in the atmosphere"
J.Atm.Sc. 20.

DRIVIERE , GANDEMER , HENRY ,(1981)
In "construire avec le vent"
NANTES C.S.T.B.

KERKER M., (1969),
"The scattering of light".
ACADEMIC PRESS.

MARTINE J.P. (1982),
"Etude experimentale de la convection naturelle entre deux plaques horizontales".
These LYON

MIE G., (1908),
Ann. Physik 25,377.

PERRIER , (1981)
personal communication

RALEIGH LORD (1899),
Phil.Mag.47,345.

SCHON J.P.,DANEL F.,MELINAND J.P.,REY C.,CHARNAY G.,
Measurment of lagrangian velocities by means of a rotating
ROLLA October 1979

SCHON J.P.,DEBBARH O.,AYRAULT M.,LADHARI F.,MEJEAN P.,PERROUX P.,GRANIER J.P.,
"Atmospheric diffusion of puffs simulation in a wind tunnel"
C.E.E.-E.D.F.-E.C.L.,report February 1984

SINCLAIR D.and LA MER V.K.,(1949)
Chem.Rev.44,245.

SNYDER W.H. and LUMLEY J.L. (1971)
"Some measuremnets of particle autocorrelation functions
in a turbulent flow".
J.F.M.48,1.

VAN DE HULST H.C., (1957)
"Light scattering by small particles".
WILEY

VEILLON F. (1981),
"private communication I.M.A.GRENOBLE".

WELLS M.H. and STOCK D.E. (1983),
"The effect of crossing trajectories on the dispersion
of particles in turbulent flow",
J.F.M. 136,1

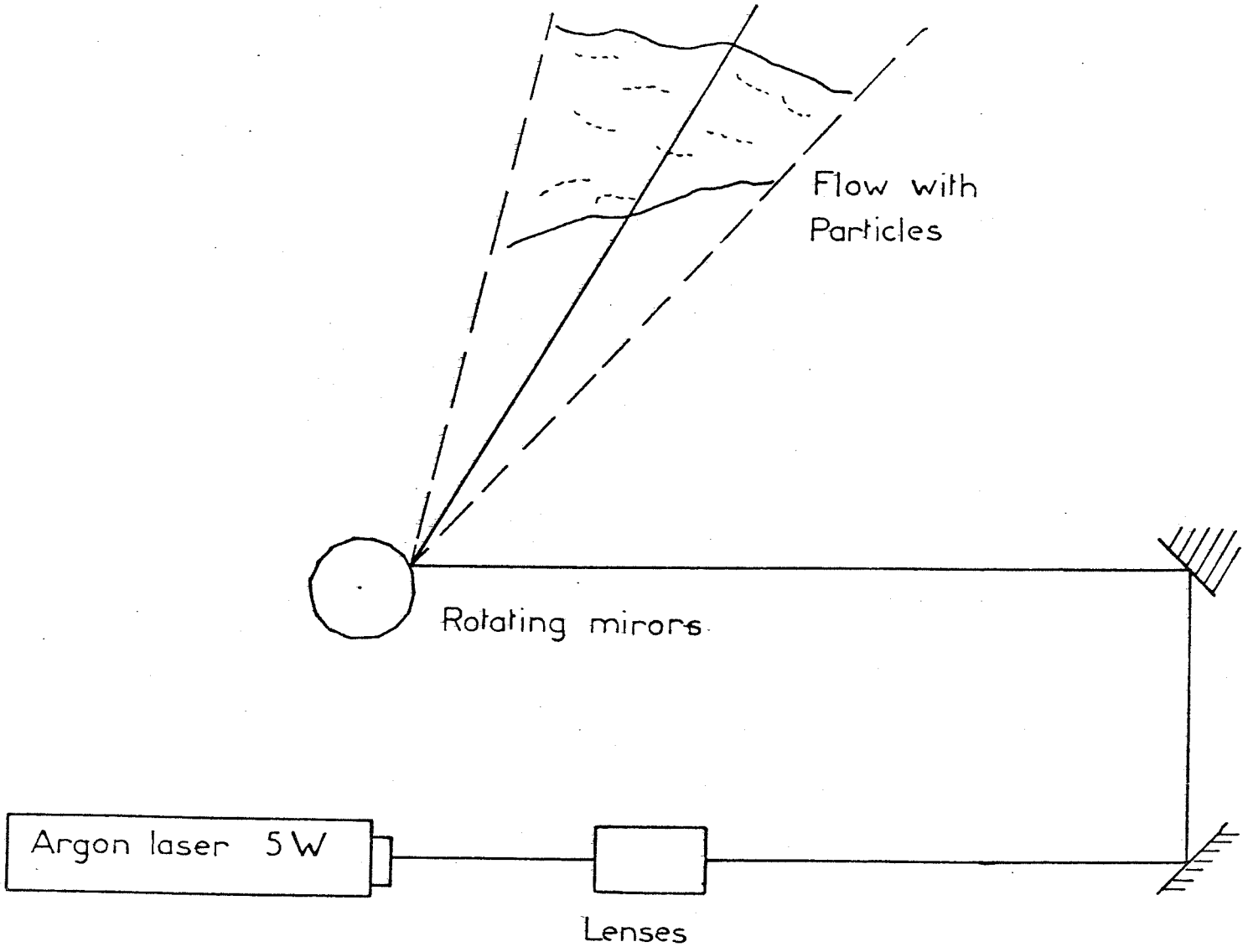
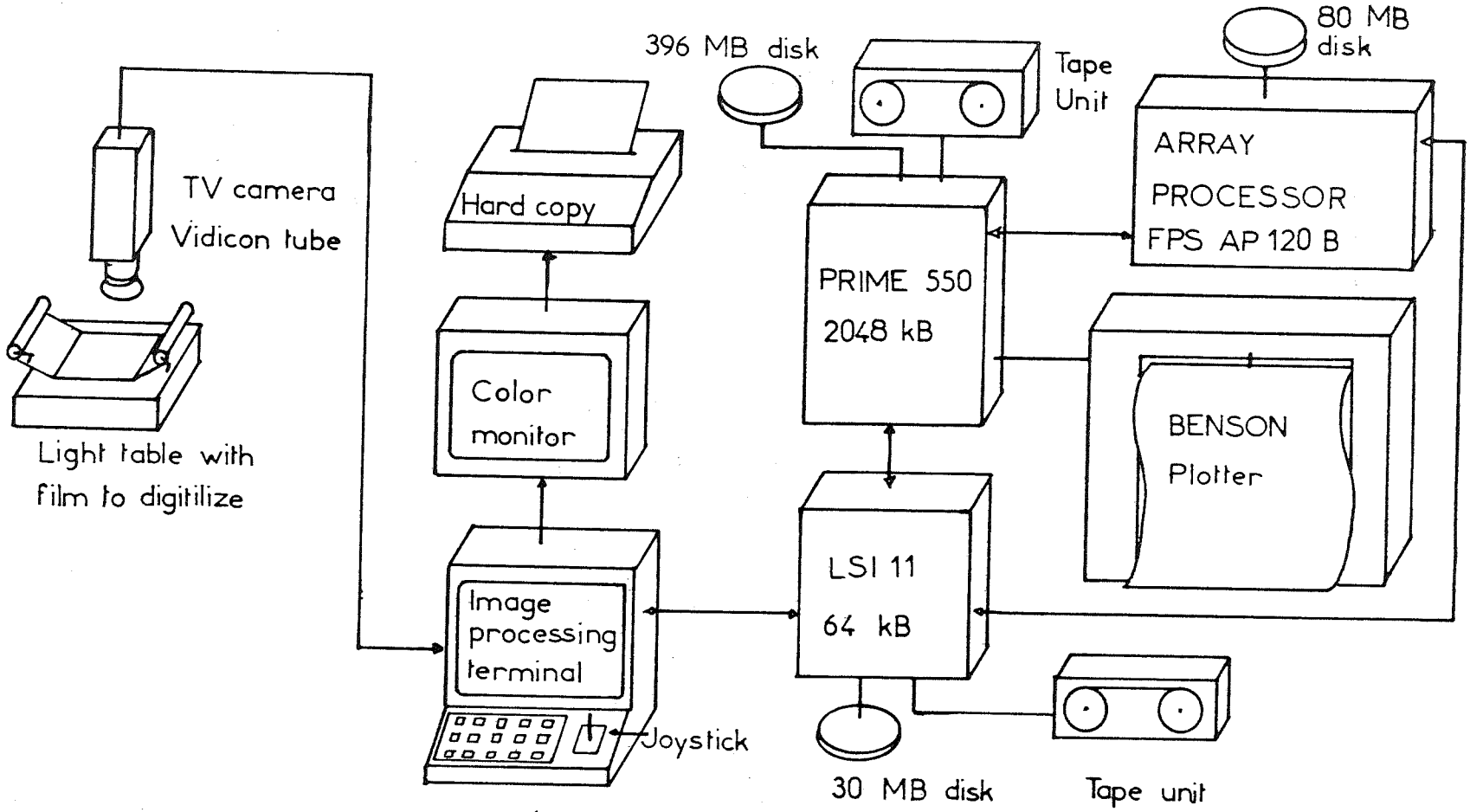
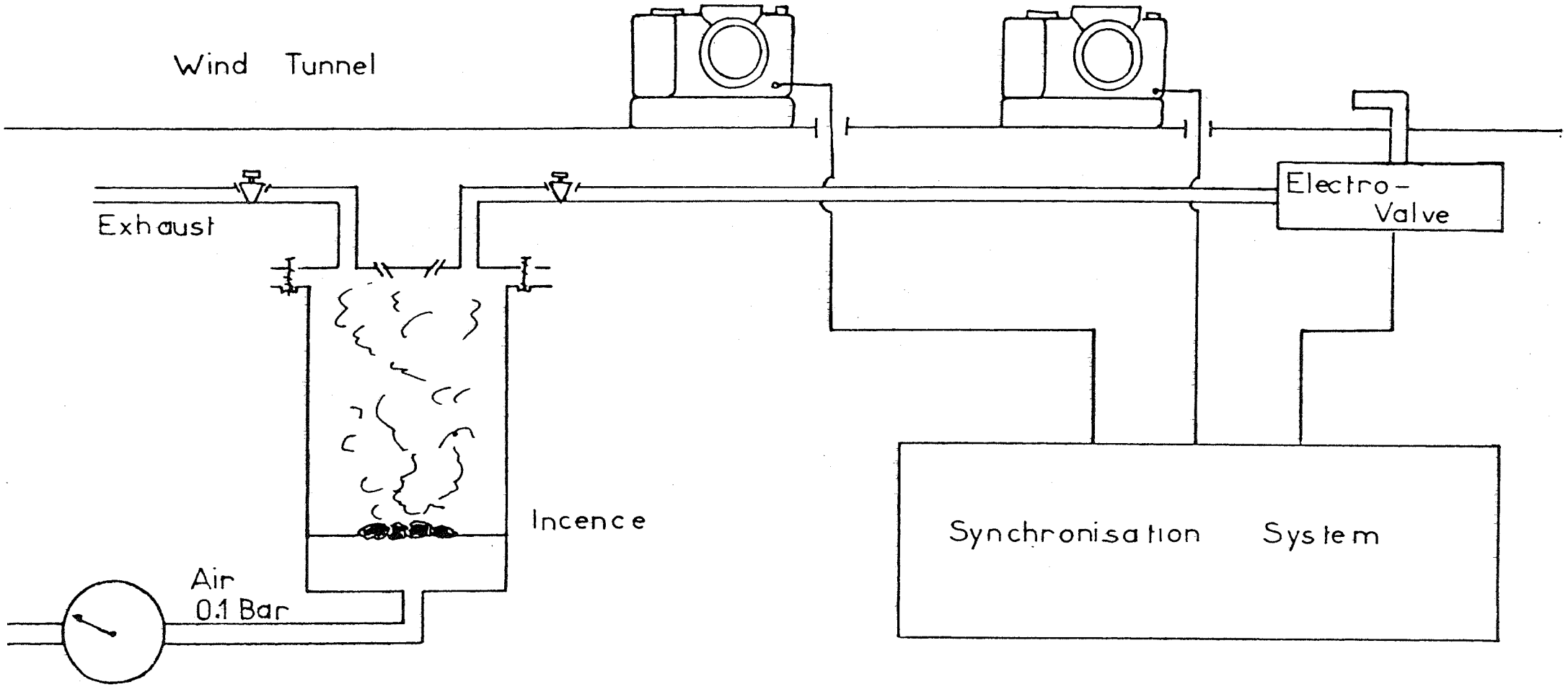


Figure 1



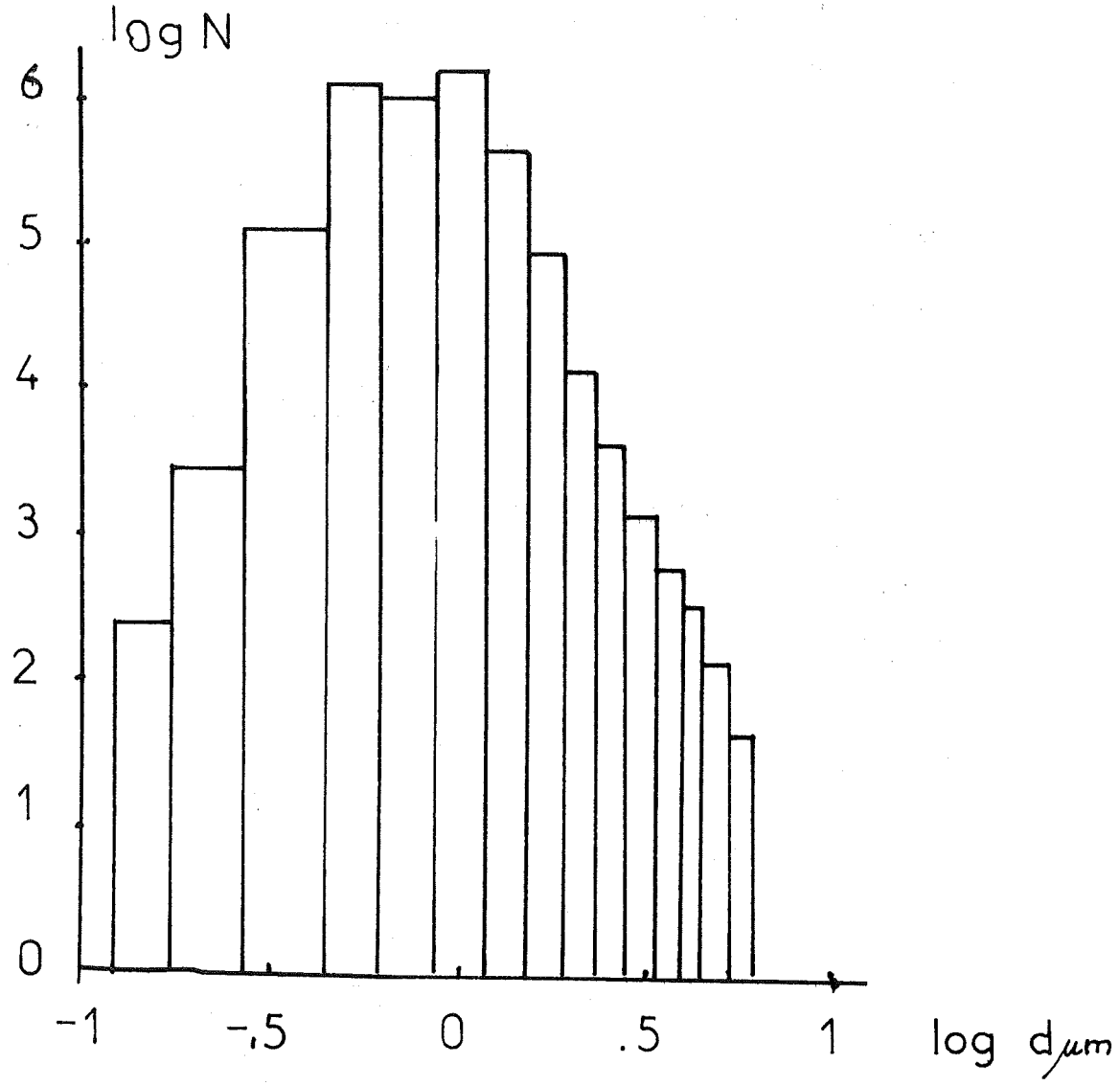
SYSTEM CONFIGURATION

Figure 2



. Injection and Photographic Systems .

Figure 3



INCENCE PARTICLES HISTOGRAM

Figure 4

Density lumination relation

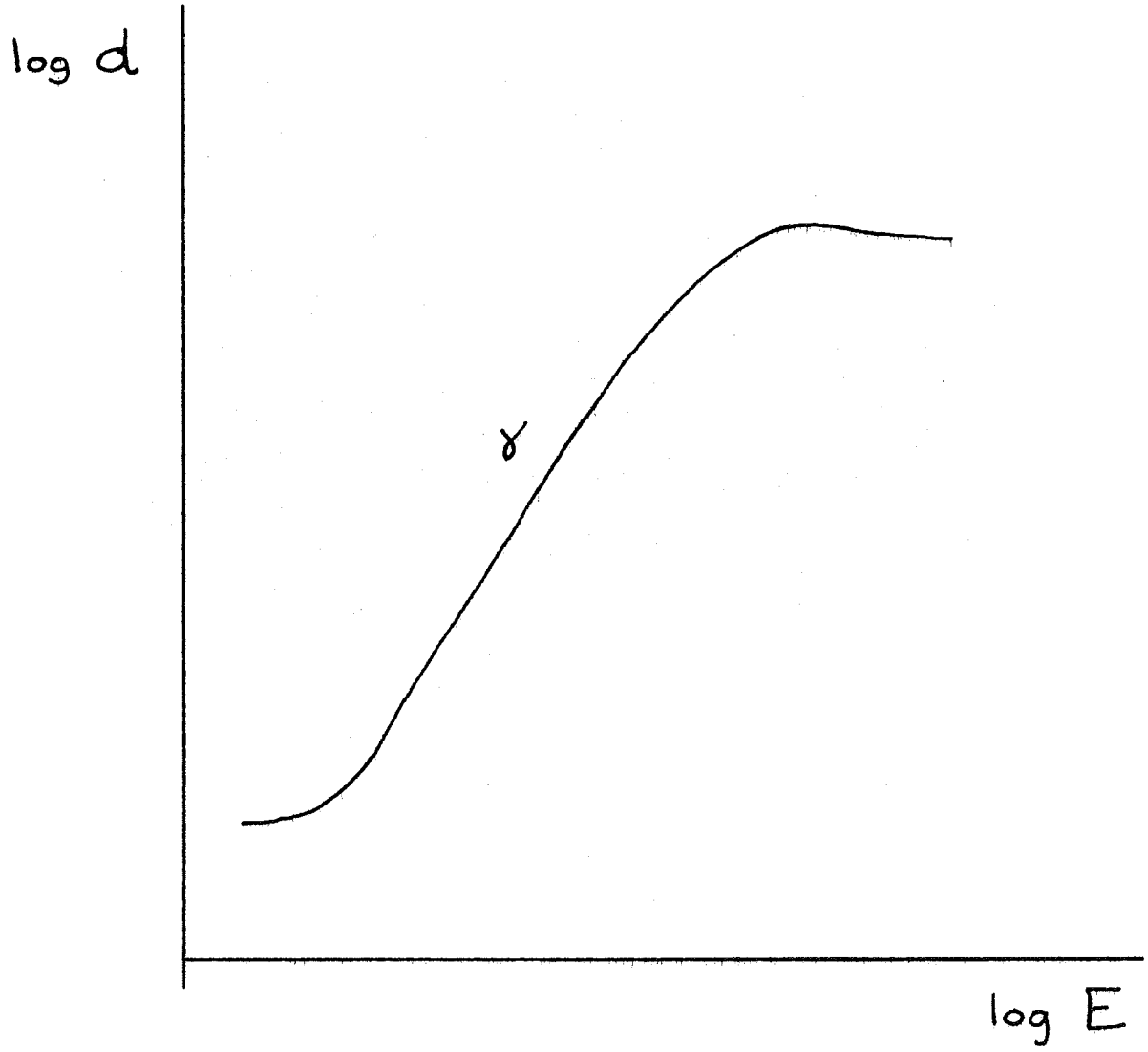
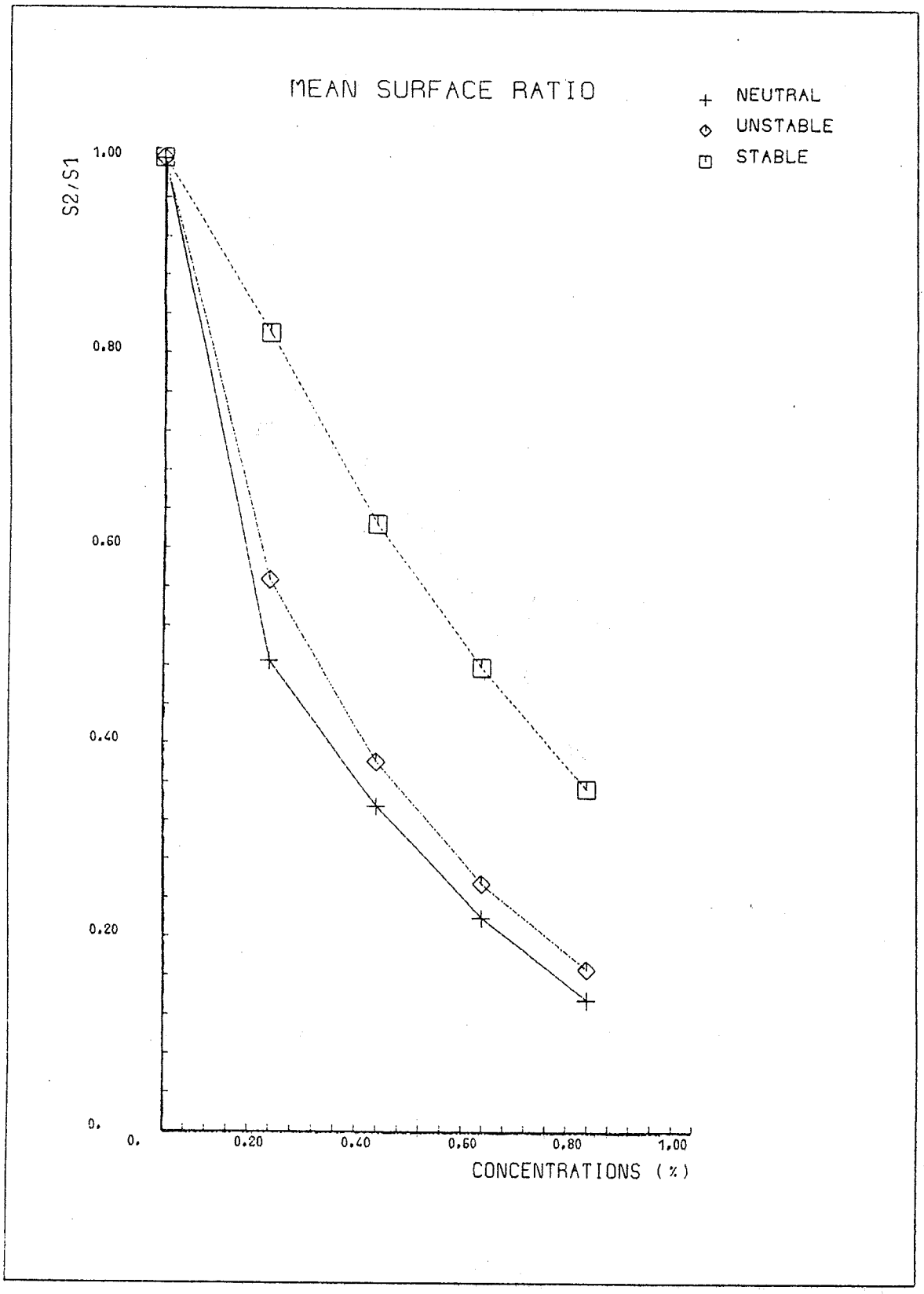
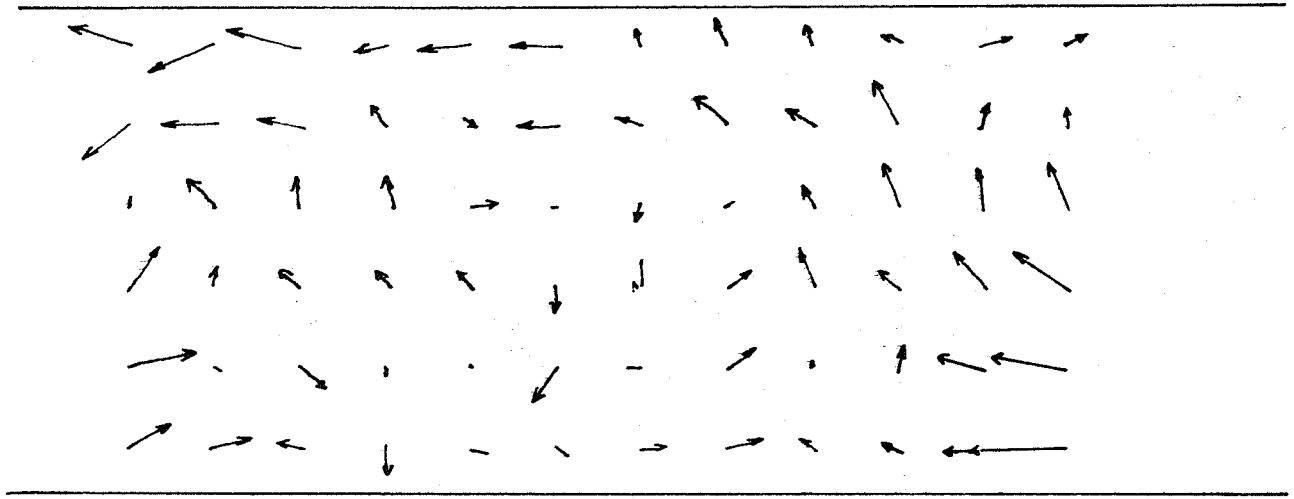


Figure 1



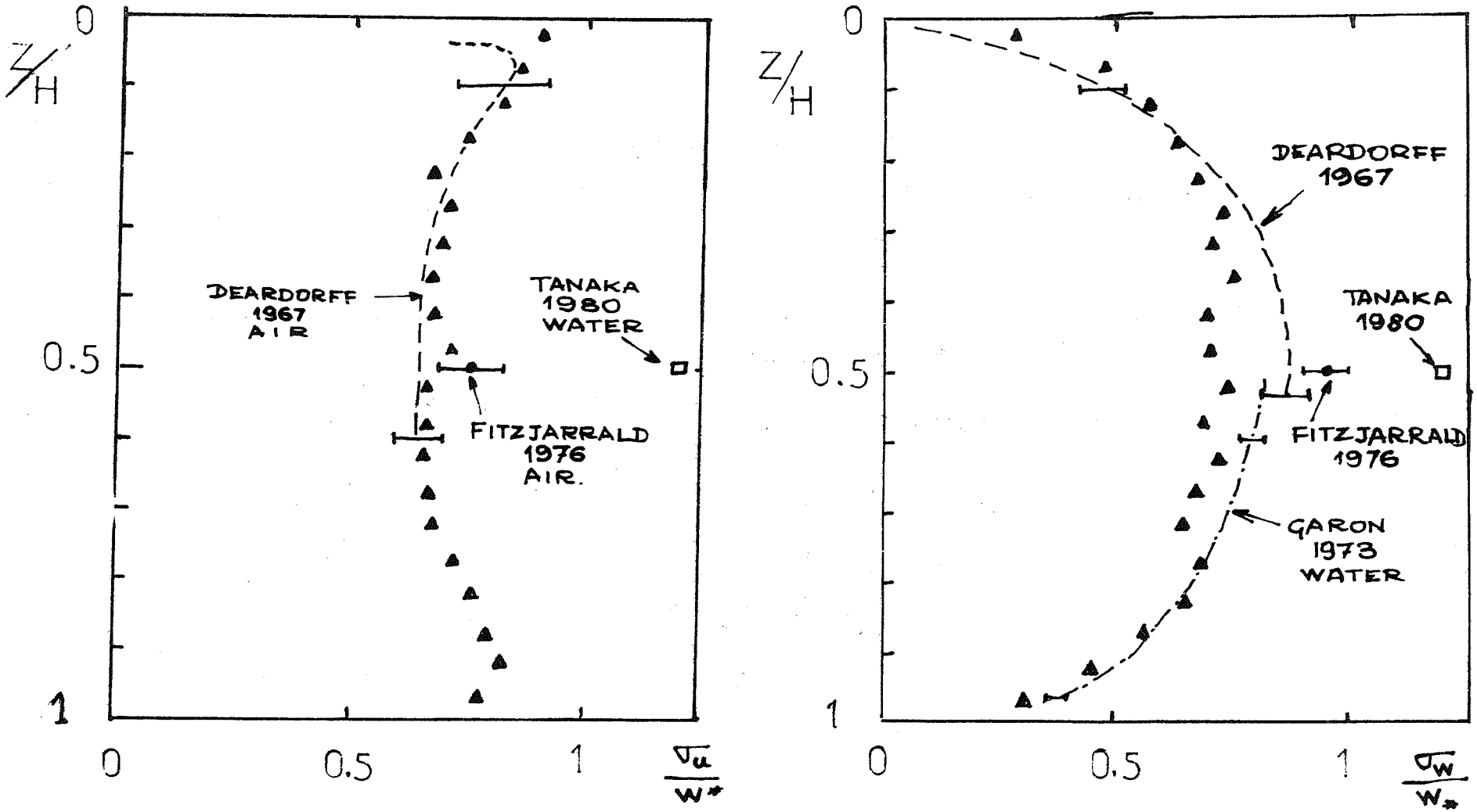
MEAN SURFACE RATIO BETWEEN 2 POSITIONS/CONCENTRATION

Figure 6



Mean Velocity Field Convection Chamber
Martine 1982

Figure 7



Comparison Of Turbulence Characteristics In Convection Chambers

Martine 1982

Figure 8

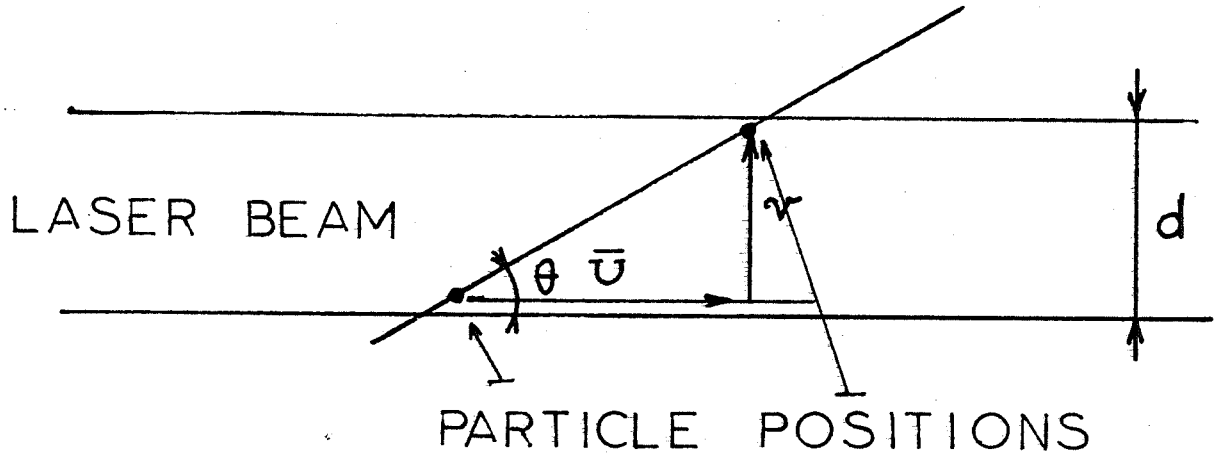


Figure 9

FREE FALL VELOCITY

dp(µm)	D.O.P. (m/s)	eau (m/s)	aloxite (m/s)
0,1	$2.72\ 10^{-7}$	$3.4\ 10^{-7}$	$9.18\ 10^{-7}$
1	$2.72\ 10^{-5}$	$3.4\ 10^{-5}$	$9.18\ 10^{-5}$
4	$4.35\ 10^{-4}$	$5.44\ 10^{-4}$	$14.7\ 10^{-3}$
10	$2.72\ 10^{-3}$	$3.4\ 10^{-3}$	$9.18\ 10^{-3}$

CARACTERISTIC TIME

dp(µm)	D.O.P. (s)	eau (s)	aloxite (s)
0,1	$2.77\ 10^{-8}$	$3.47\ 10^{-8}$	$1.37\ 10^{-8}$
1	$2.77\ 10^{-6}$	$3.47\ 10^{-6}$	$9.37\ 10^{-6}$
4	$4.44\ 10^{-5}$	$5.55\ 10^{-5}$	$1.5\ 10^{-5}$
10	$2.77\ 10^{-4}$	$3.47\ 10^{-4}$	$9.37\ 10^{-4}$

TABLE 1

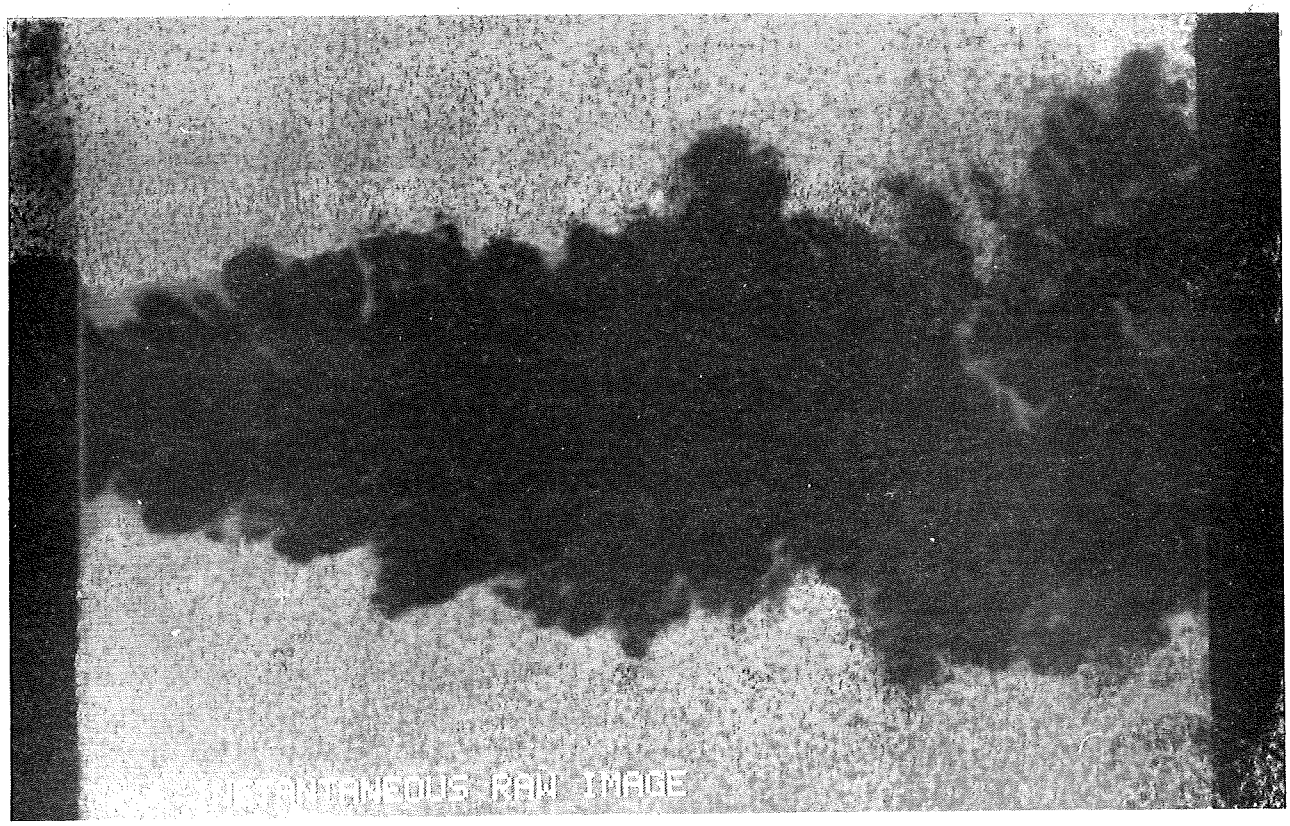


PHOTO N° 1

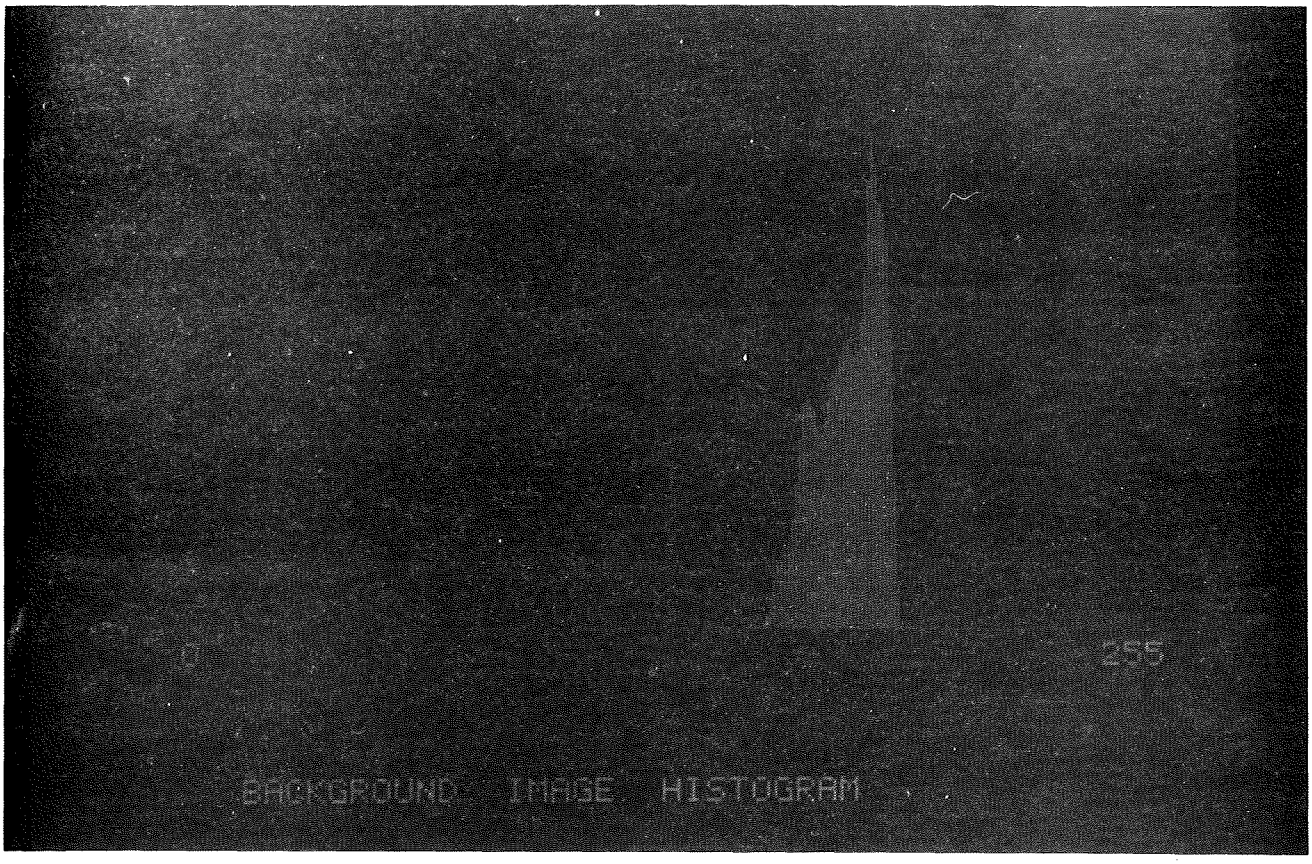


PHOTO N° 2

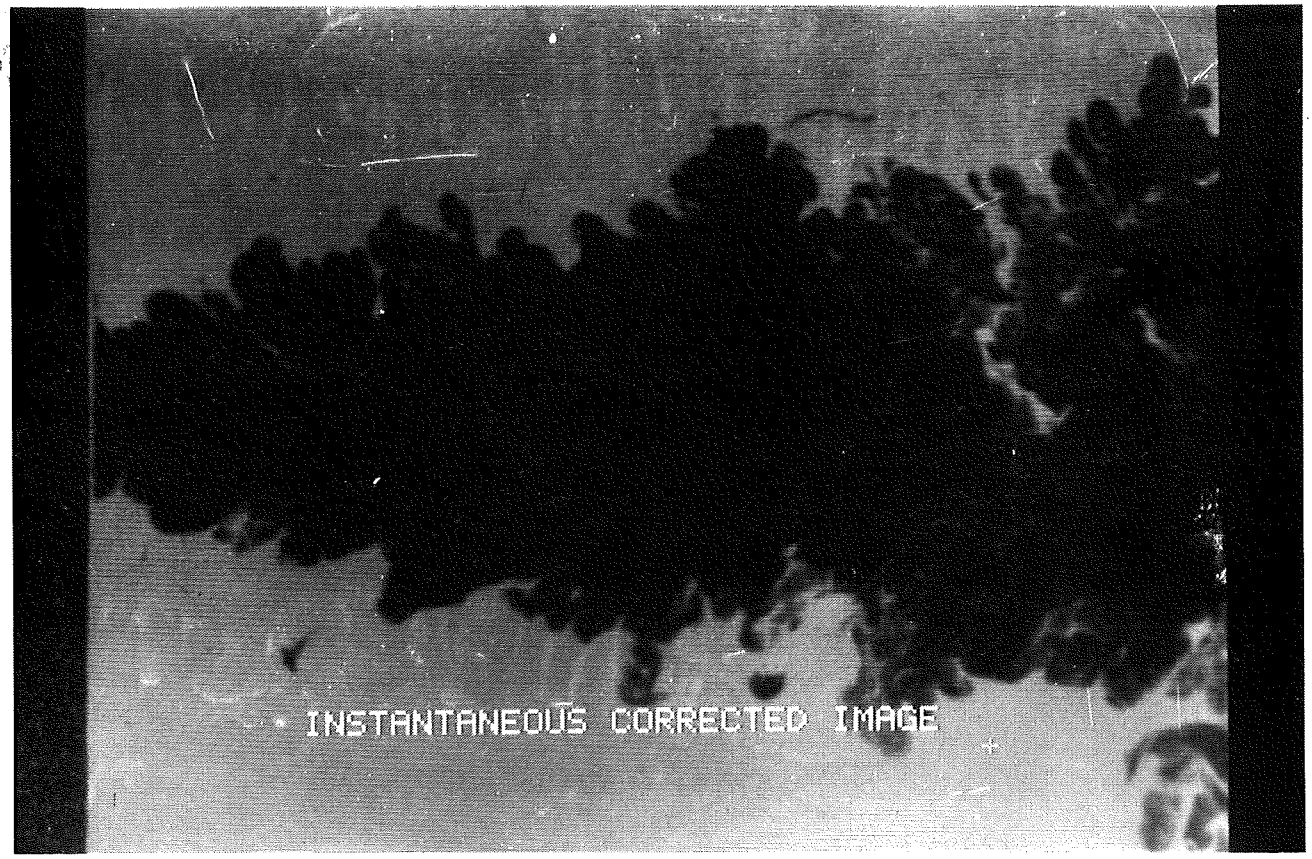


PHOTO N° 3

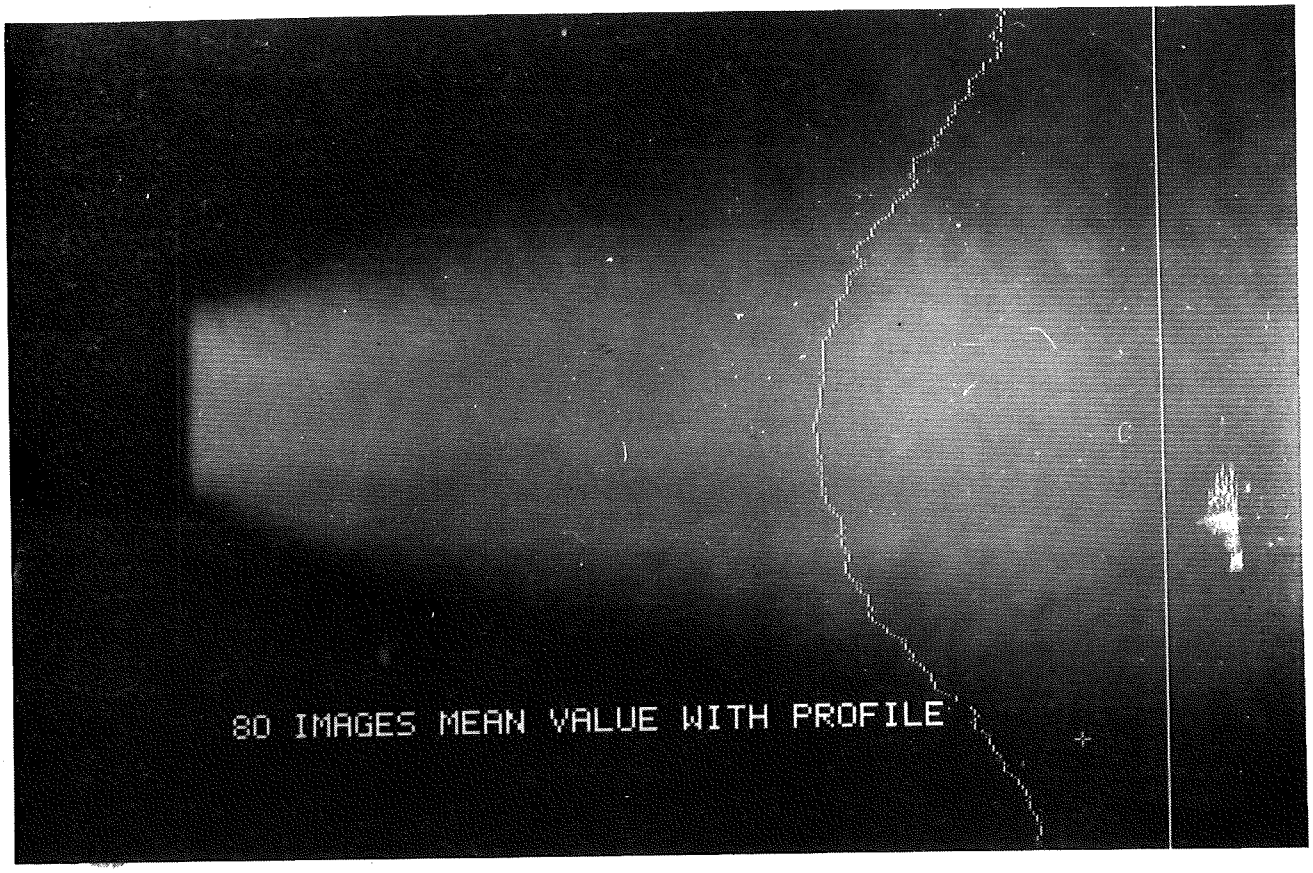


PHOTO N° 4

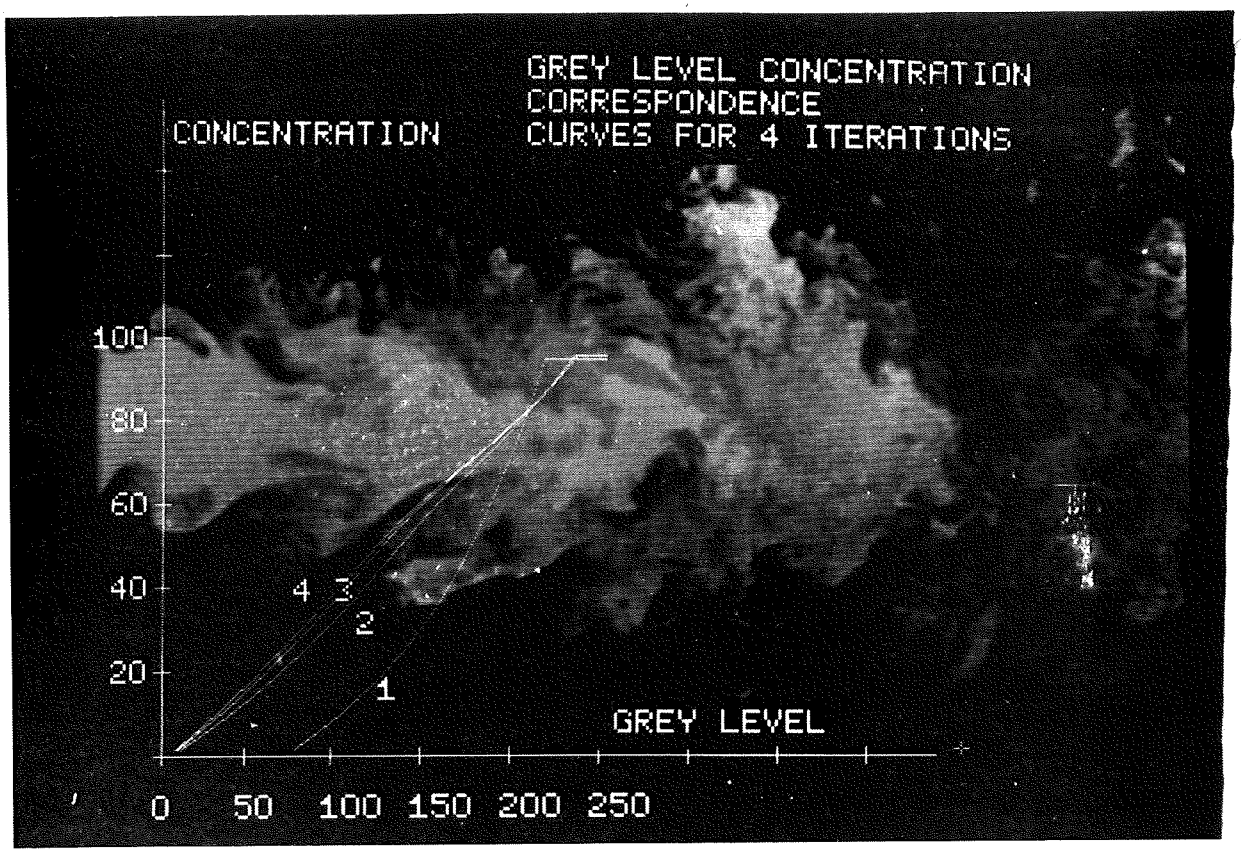


PHOTO N° 5

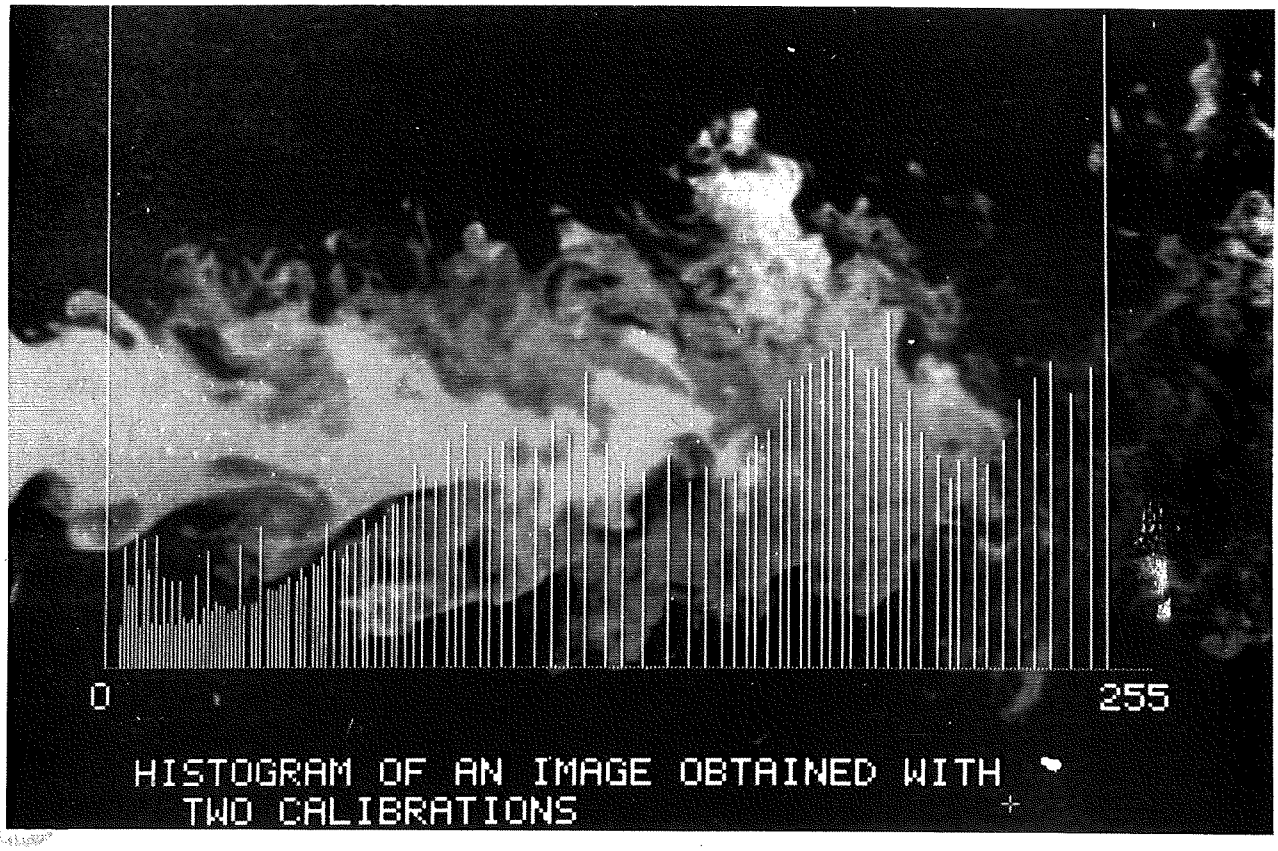


PHOTO N° 6

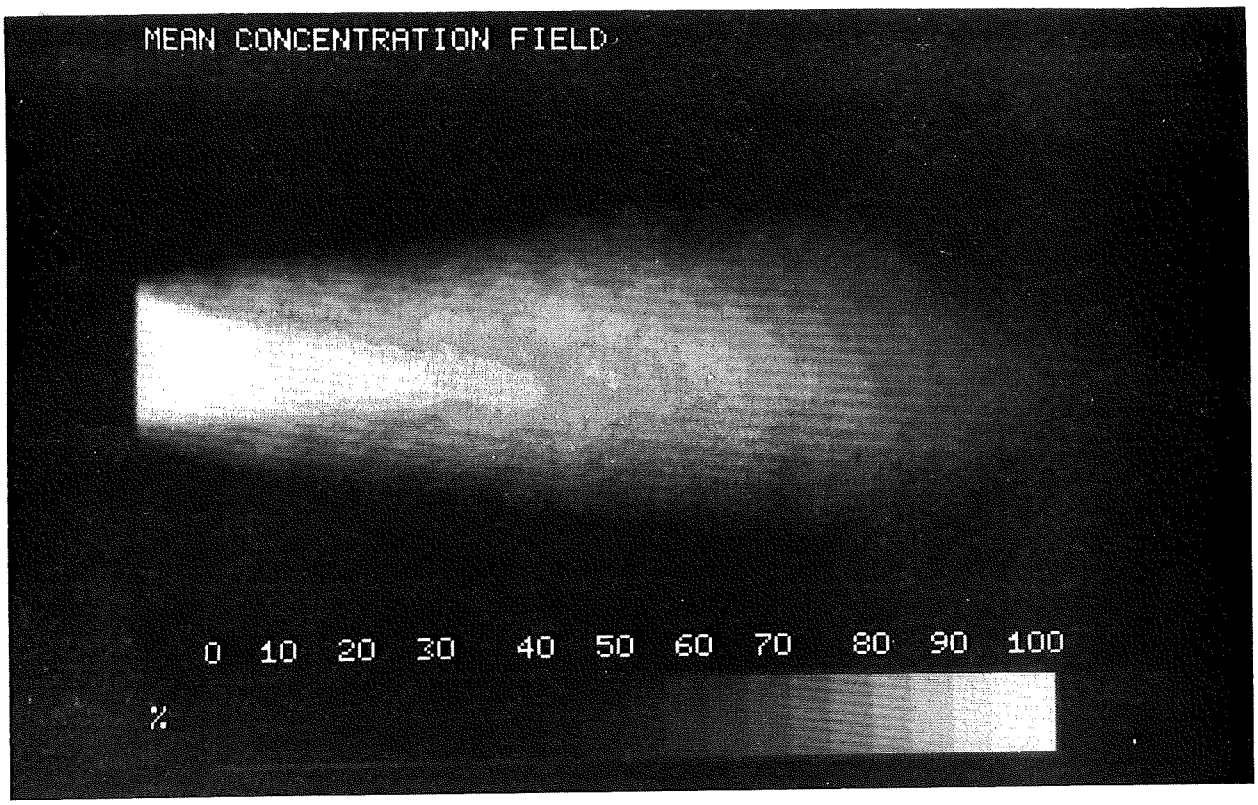


PHOTO N° 7

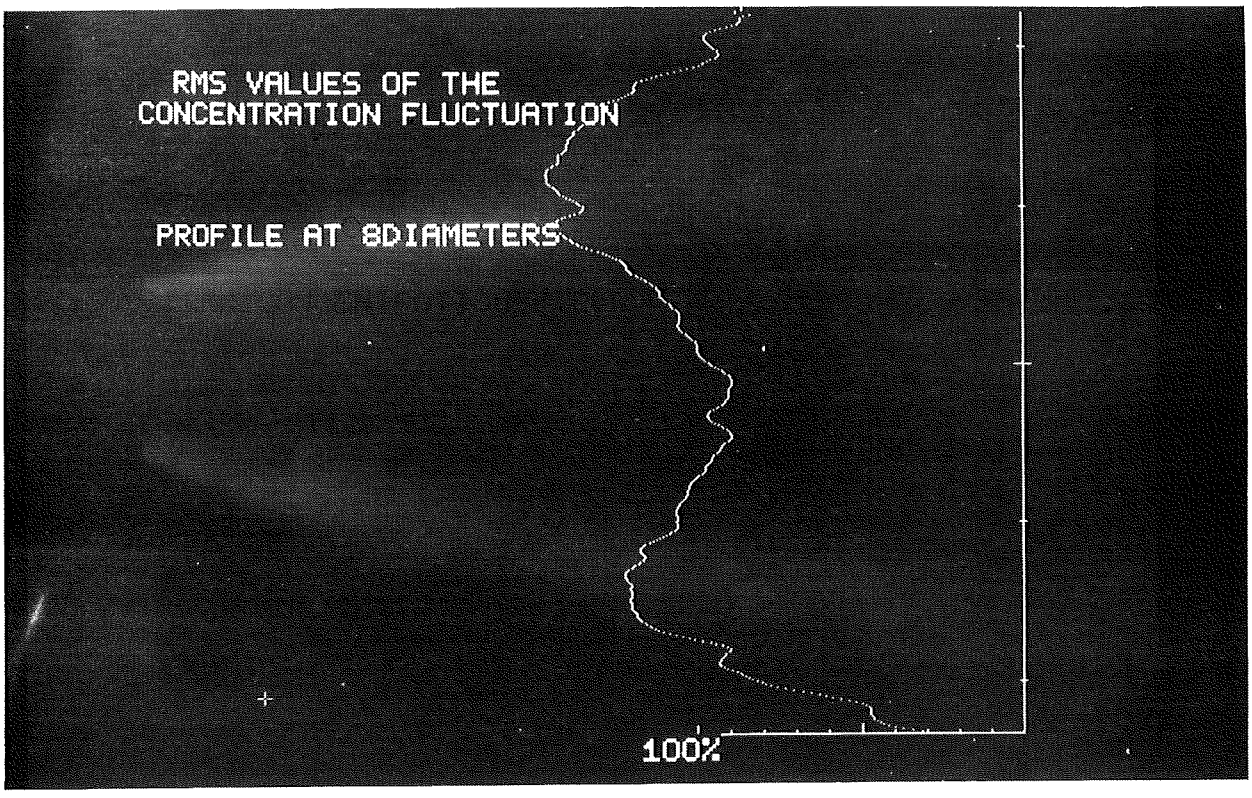


PHOTO N° 8

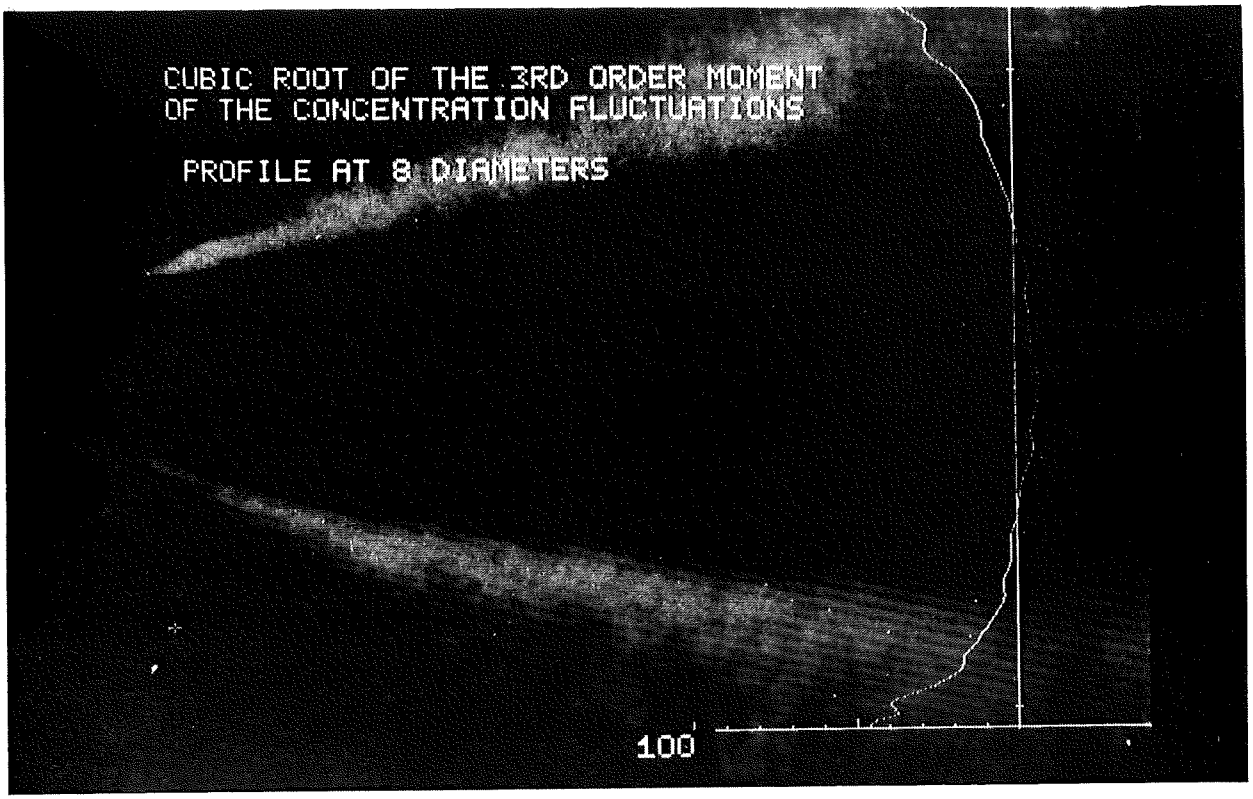

CUBIC ROOT OF THE 3RD ORDER MOMENT
OF THE CONCENTRATION FLUCTUATIONS
PROFILE AT 8 DIAMETERS
100

PHOTO N° 9

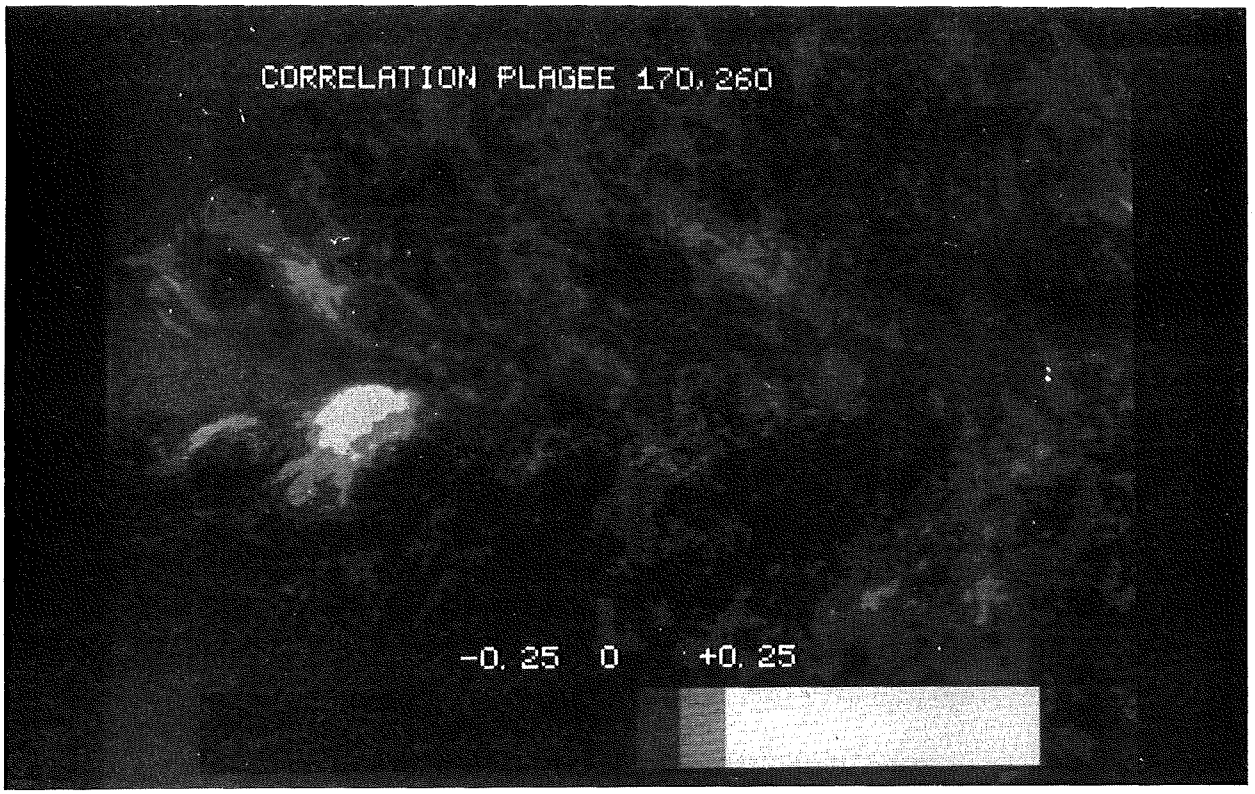


PHOTO N° 10

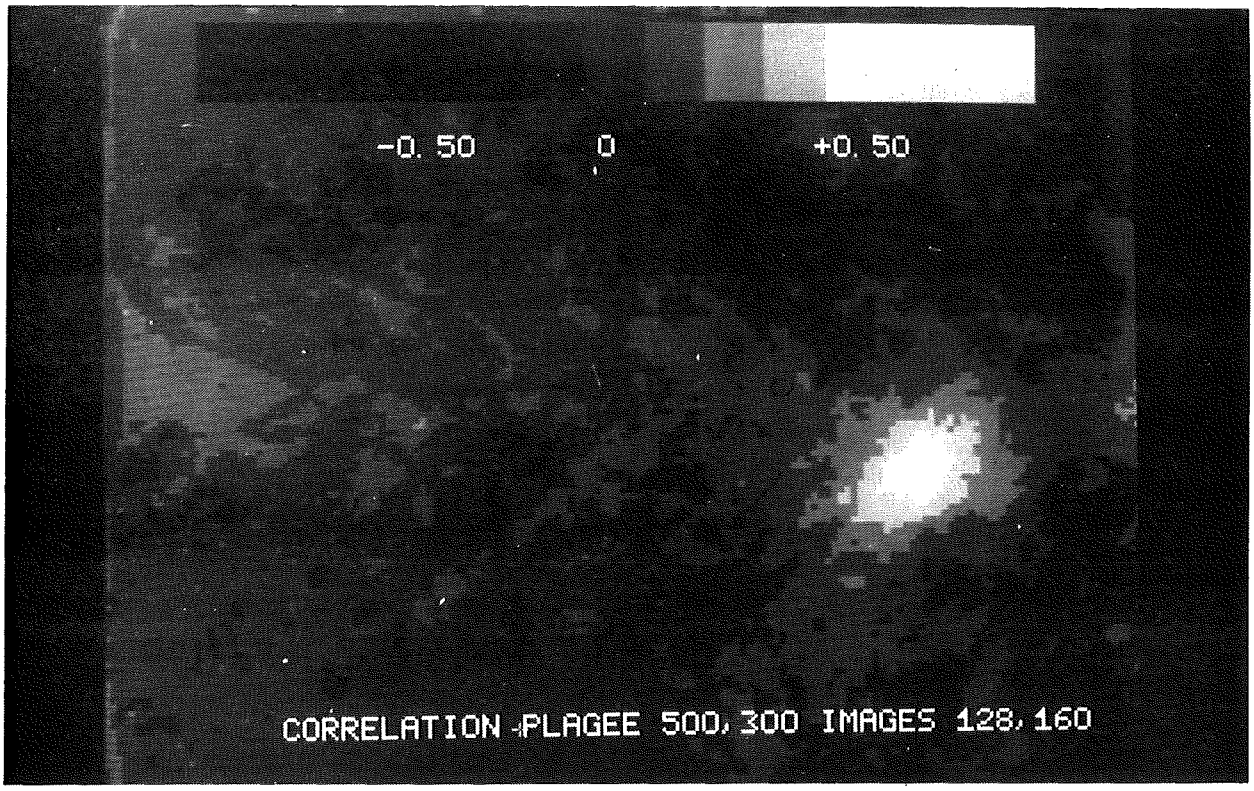


PHOTO N° 11

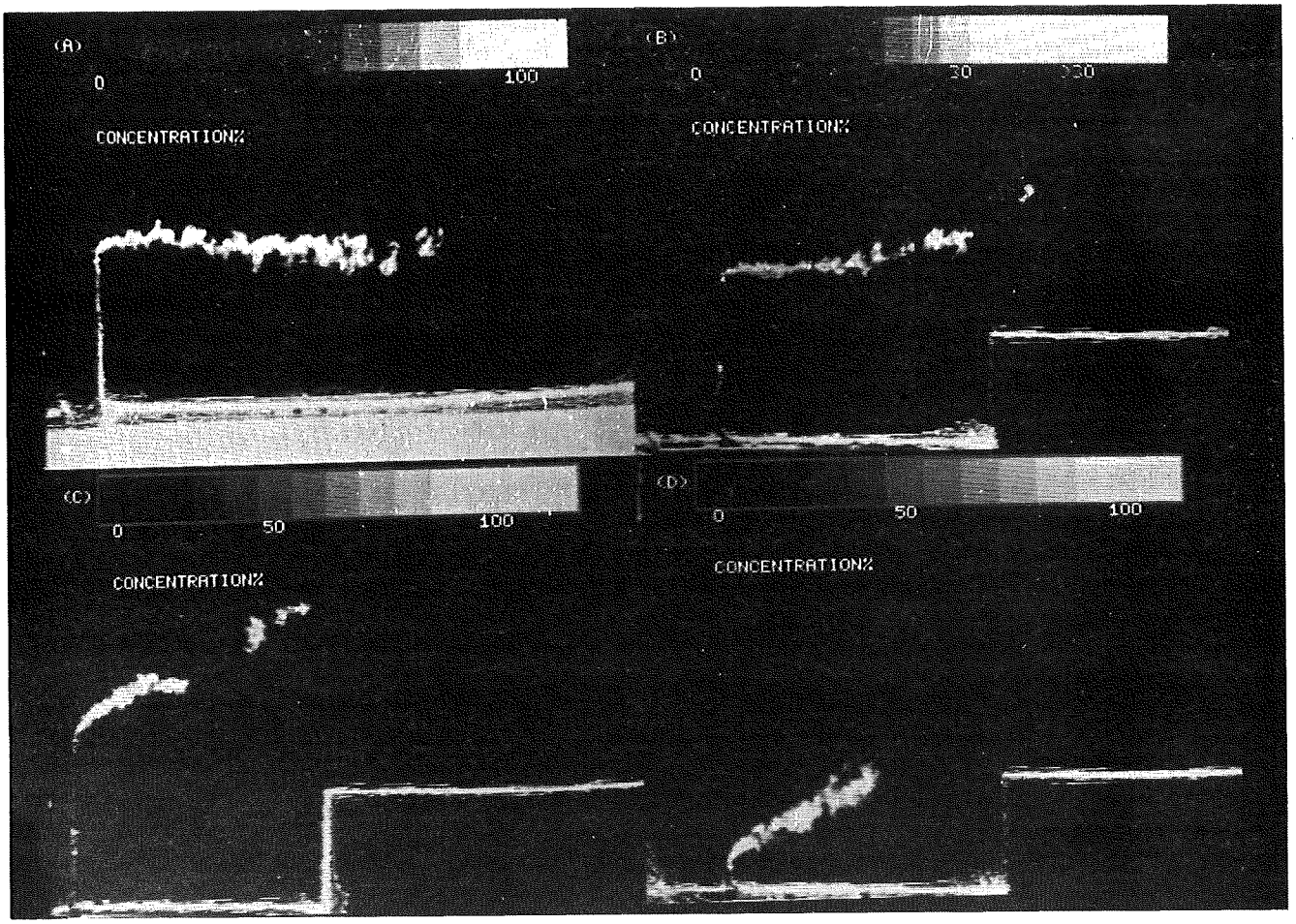


PHOTO N° 12

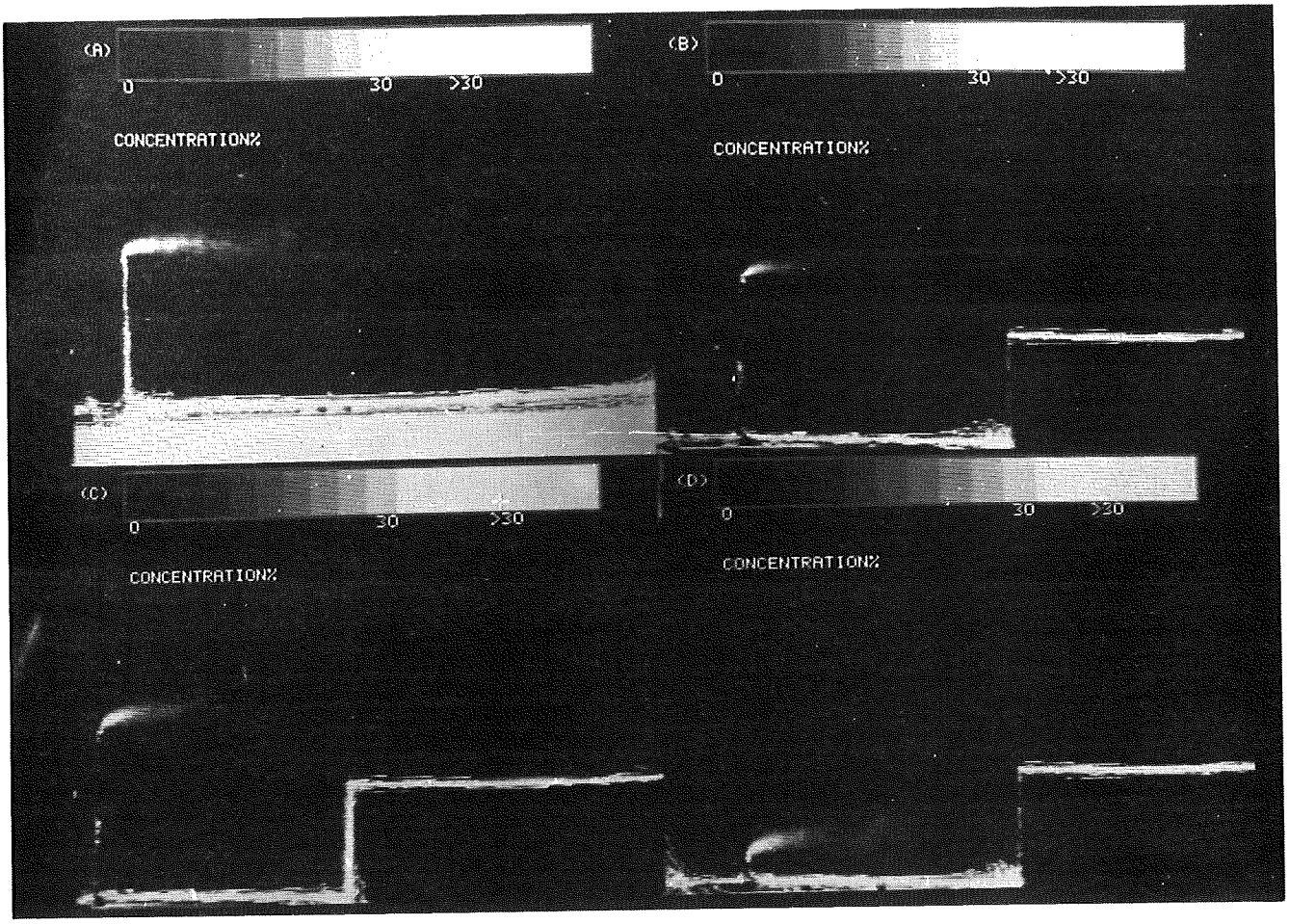


PHOTO N° 13

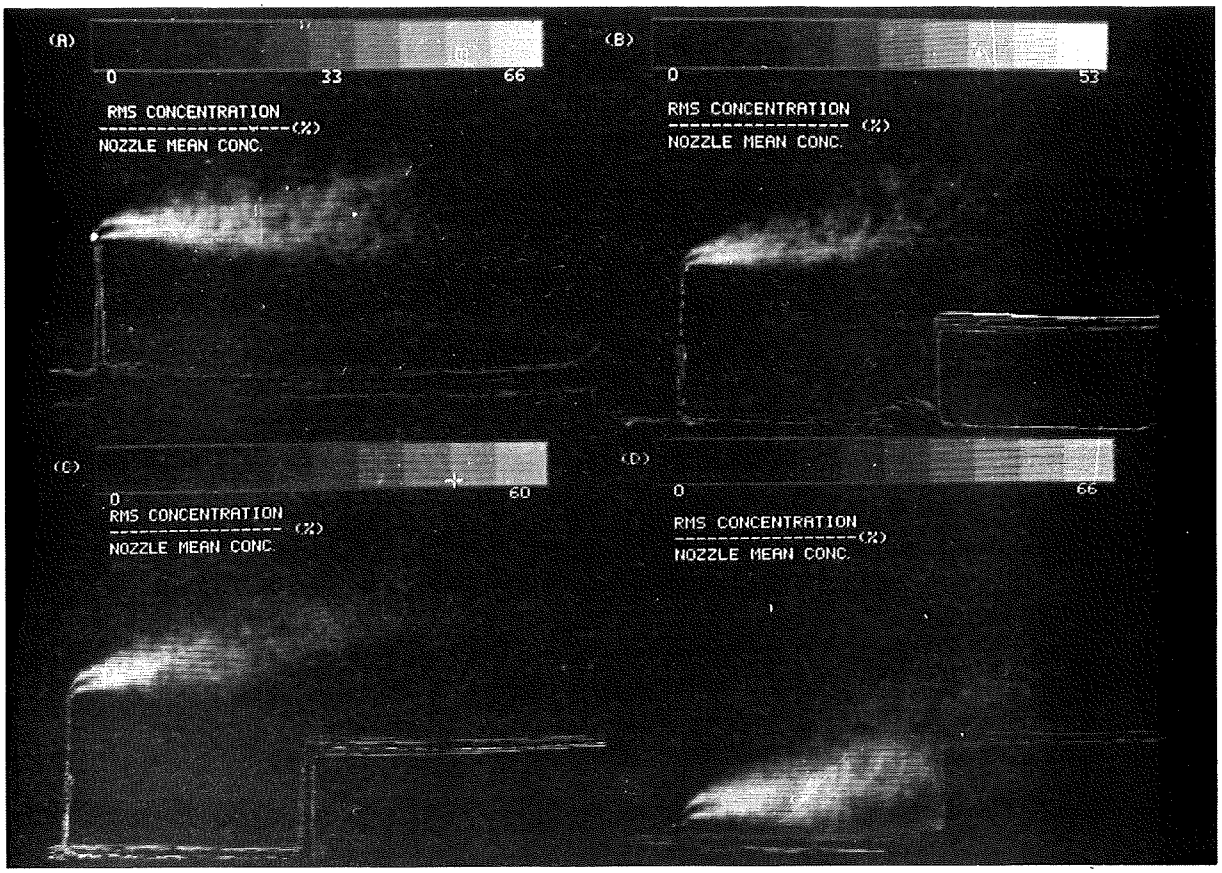


PHOTO N° 14

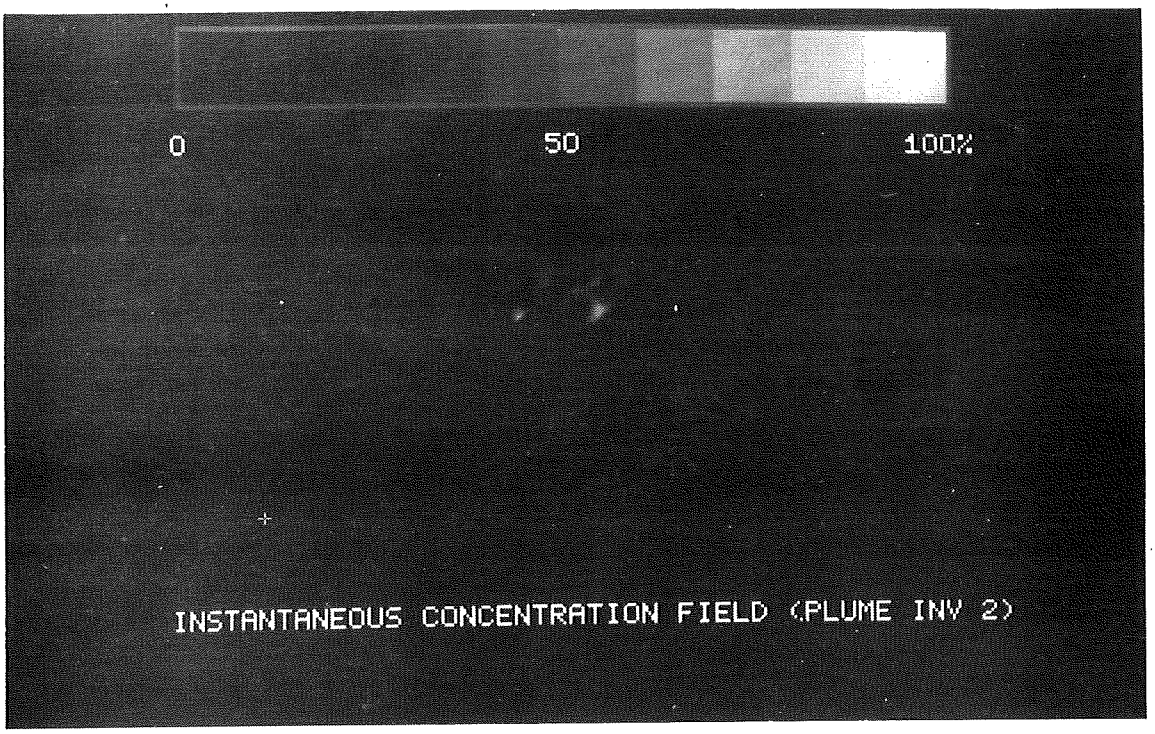


PHOTO N° 15

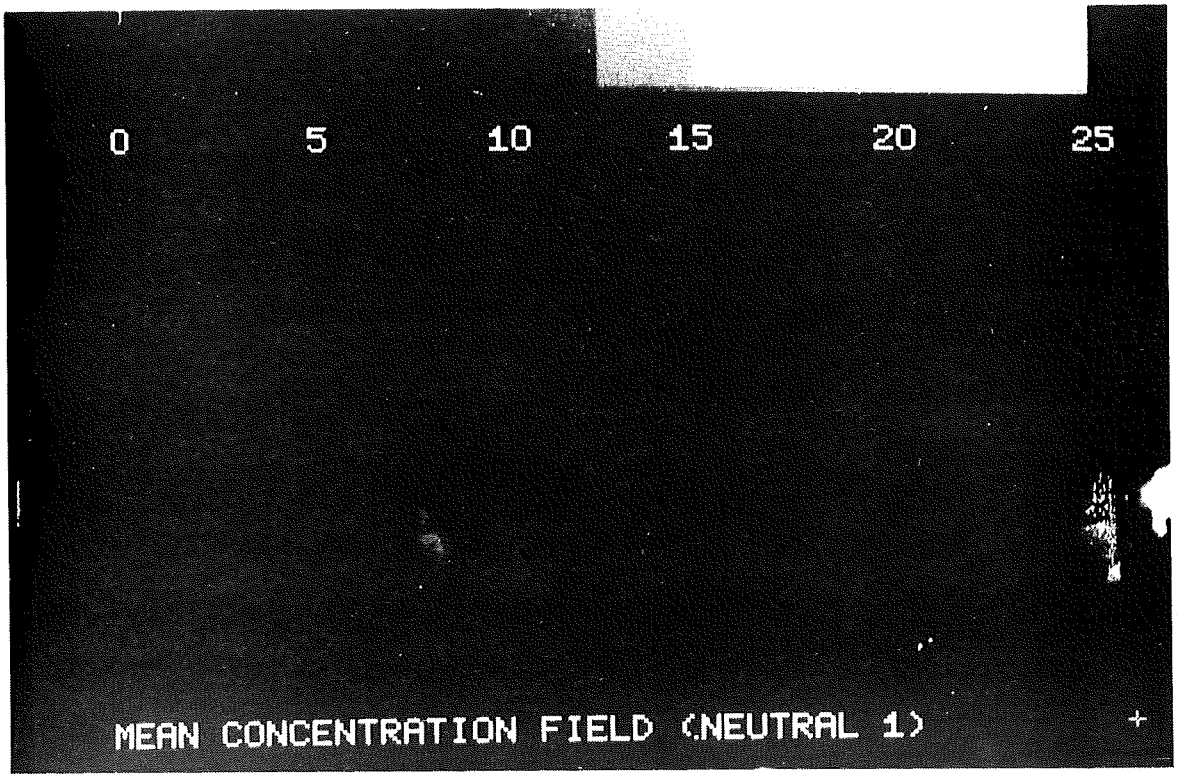


PHOTO N° 16

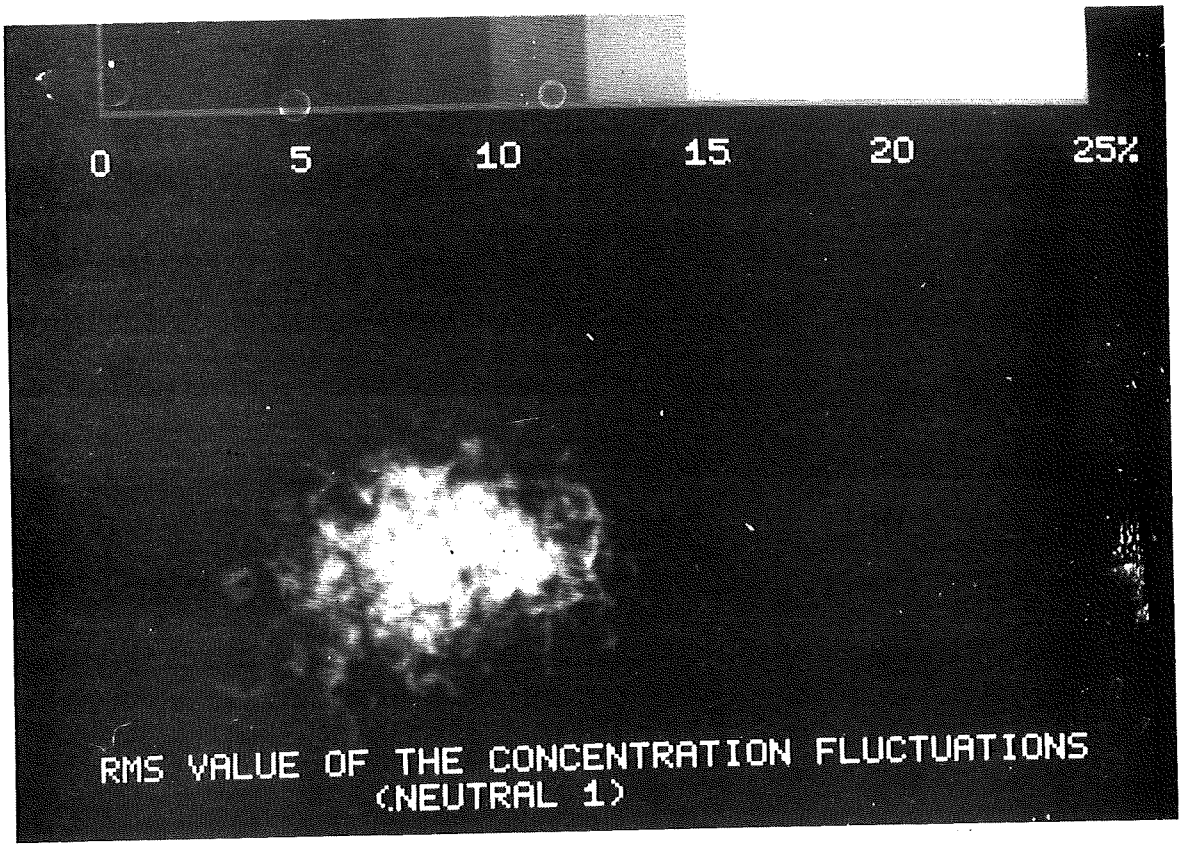


PHOTO N° 17

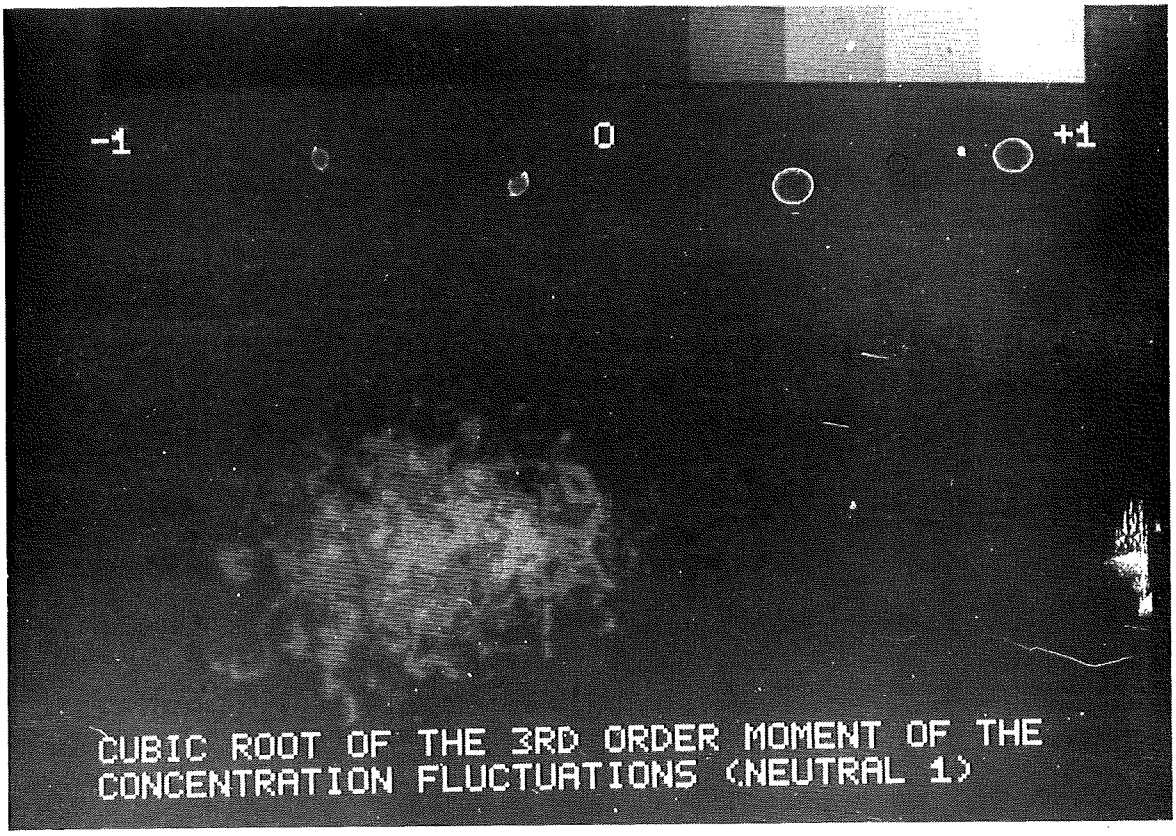


PHOTO N° 18



PHOTO N° 19

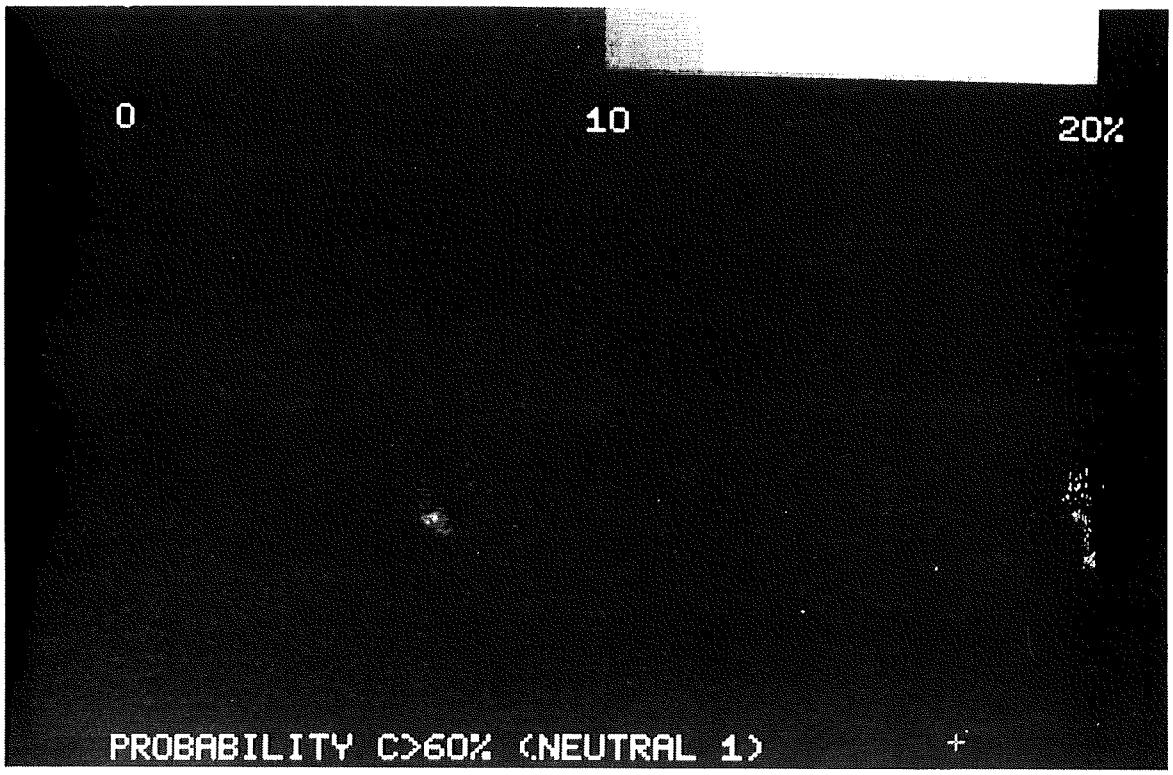


PHOTO N° 20



PHOTO N° 21



PHOTO N° 22

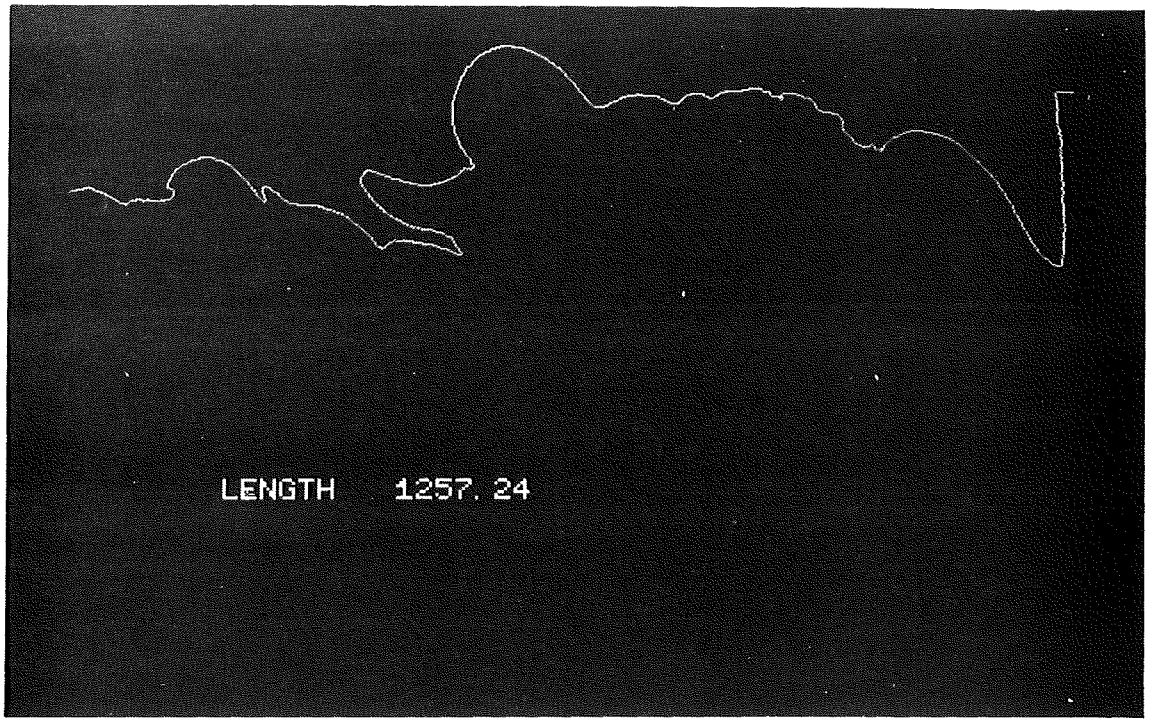


PHOTO N° 23

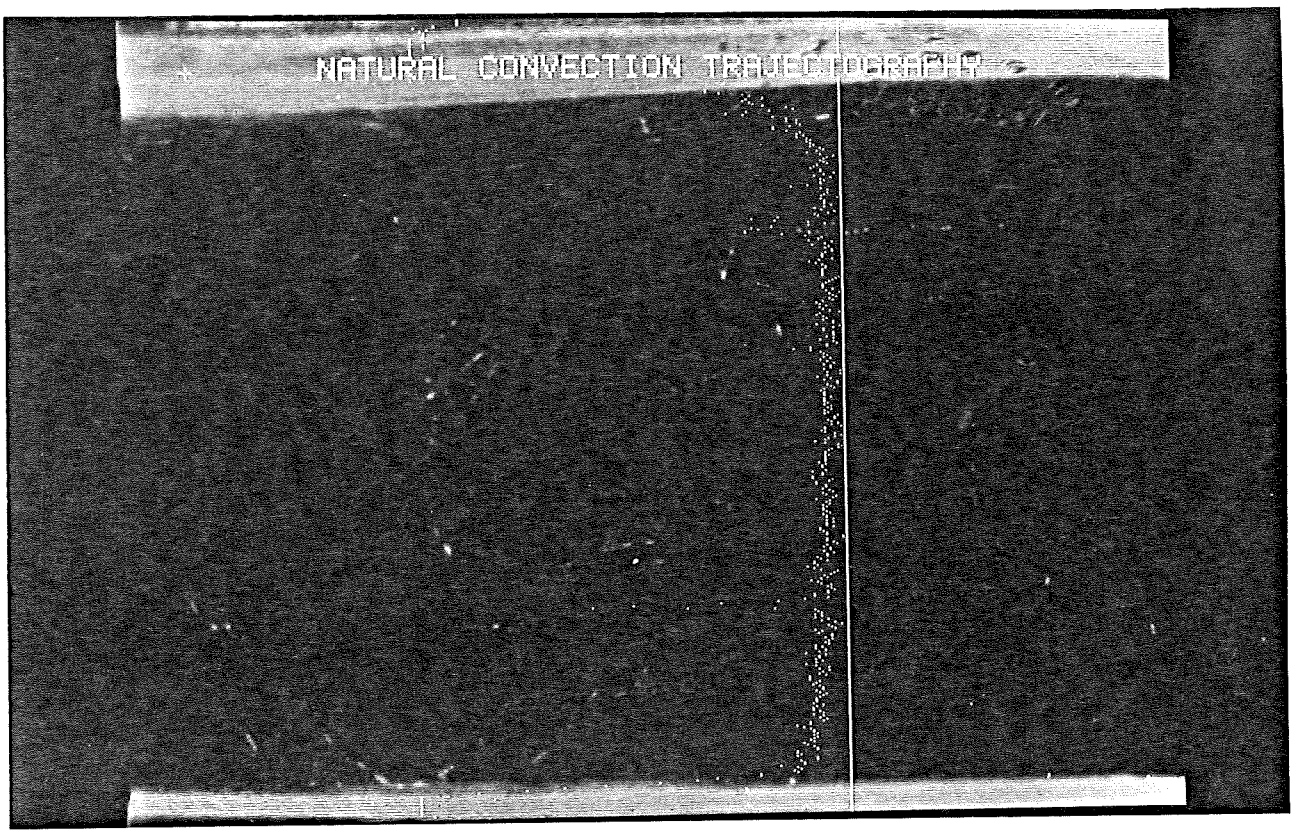


PHOTO N° 24

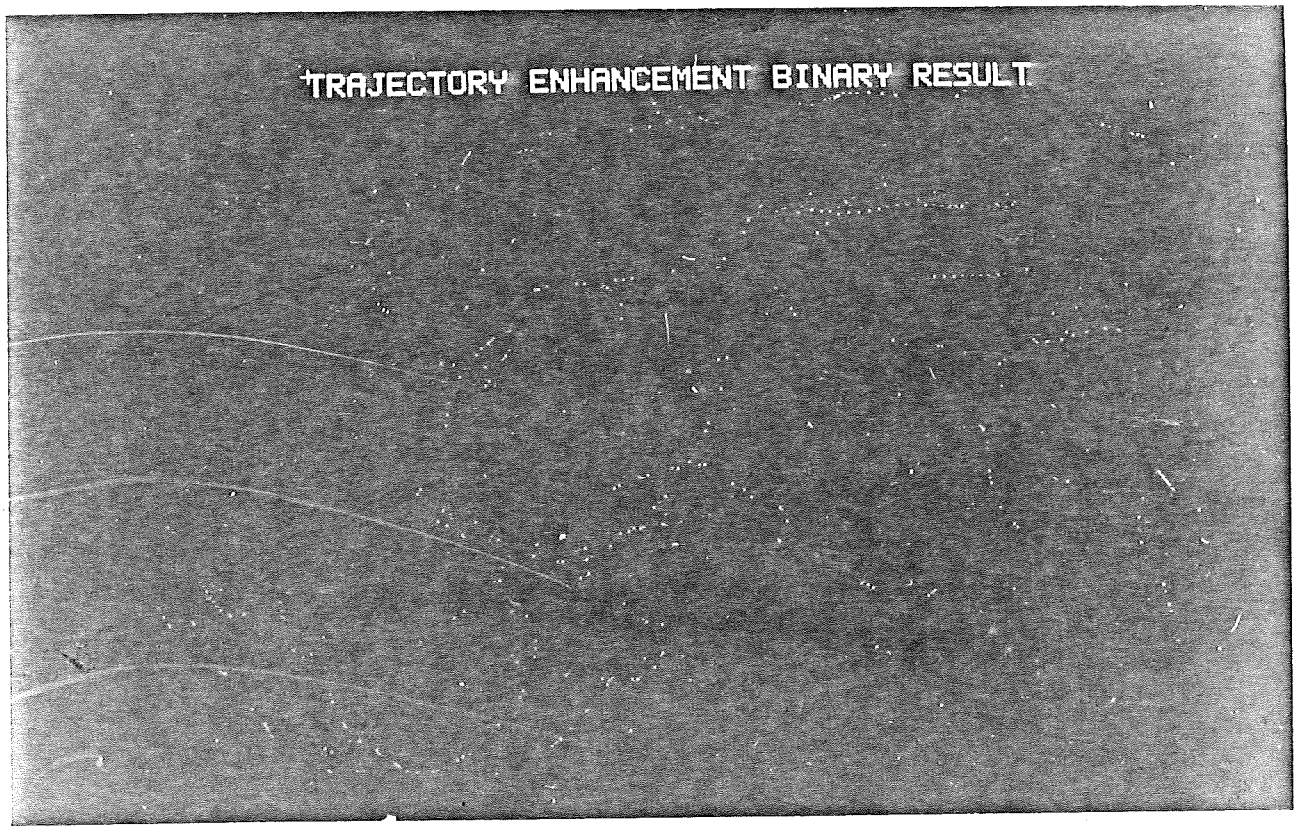


PHOTO N° 25

